This document is confidential and is proprietary to the American Chemical Society and its authors. Do not copy or disclose without written permission. If you have received this item in error, notify the sender and delete all copies.

Designed glycopeptidomimetics disrupt protein-protein interactions mediating amyloid β-peptide aggregation and restore neuroblastoma cell viability

Journal:	*Journal of Medicinal Chemistry*
Manuscript ID	jm-2015-016292.R1
Manuscript Type:	Article
Date Submitted by the Author:	n/a

Complete List of Authors:	Kaffy, Julia; Université Paris Sud, UMR CNRS 8076 Brinet, Dimitri; Université Paris Sud, UMR CNRS 8076 Soulier, Jean-Louis; Université Paris Sud, UMR CNRS 8076 Correia, Isabelle; UPMC Univ Paris 06, Laboratoire des Biomolécules, UMR 7203 CNRS-UPMC-ENS Tonali, Nicolo; Université Paris Sud, UMR CNRS 8076 Fera, Katia ; Université Paris Sud, UMR CNRS 8076 Iacone, Yasmine; UMR CNRS 8612-institut Galien Paris Sud, Laboratoire des proteines et nanotechnologies en sciences analytiques Hoffmann, Anaïs; UPMC Univ Paris 06, Laboratoire des Biomolécules, UMR 7203 CNRS-UPMC-ENS Khemtémourian, Lucie; UPMC Univ Paris 06, Laboratoire des Biomolécules, UMR 7203 CNRS-UPMC-ENS Crousse, Benoit; cnrs, BioCIS / UMR 8076 Taylor, Mark; Lancaster University, Biomedical and Life Sciences Allsop, David; Lancaster University, Biomedical and Life Sciences Taverna, Myriam; UMR CNRS 8612-institut Galien Paris Sud, Laboratoire des proteines et nanotechnologies en sciences analytiques Lequin, Olivier; University Pierre and Marie Curie, UMR 7613 CNRS-UPMC Ongeri, Sandrine; Université Paris Sud, UMR CNRS 8076

SCHOLARONE™
Manuscripts

1 2 3 4 5 6 7 8 9 10 11 12 13 14 15 16 17 18 19 20 21 22 23 24 25 26 27 28 29 30 31 32 33 34 35 36 37 38 39 40 41 42 43 44 45 46 47 48 49 50 51 52 53 54 55 56 57 58 59 60

Designed glycopeptidomimetics disrupt protein-protein interactions mediating amyloid β-peptide aggregation and restore neuroblastoma cell viability

Julia Kaffy[1], Dimitri Brinet[1,2], Jean-Louis Soulier[1], Isabelle Correia[3], Nicolo Tonali[1], Katia Fabiana Fera[1], Yasmine Iacone[1,2], Anaïs R. F. Hoffmann[3], Lucie Khemtémourian[3], Benoit Crousse[1], Mark Taylor[4], David Allsop[4], Myriam Taverna,[2] Olivier Lequin[3], Sandrine Ongeri[1]*

[1]Molécules Fluorées et Chimie Médicinale, BioCIS, Univ. Paris-Sud, CNRS, Université Paris Saclay, 5 rue Jean-Baptiste Clément, 92296 Châtenay-Malabry Cedex, France

[2]Protéines et Nanotechnologies en Sciences Séparatives, Institut Galien Paris-Sud, Univ. Paris-Sud, CNRS, Université Paris Saclay, 5 rue Jean-Baptiste Clément, 92296 Châtenay-Malabry Cedex, France

[3]Sorbonne Universités - UPMC Univ Paris 06, Ecole Normale Supérieure - PSL Research University, CNRS UMR 7203 LBM, 4 place Jussieu, 75252 Paris Cedex 05, France

[4]Lancaster University, Division of Biomedical and Life Sciences, Faculty of Health and Medicine, Lancaster LA1 4YQ, UK

1
2
3
4
5
6
7
8
9
10
11
12
13
14
15
16
17
18
19
20
21
22
23
24
25
26
27
28
29
30
31
32
33
34
35
36
37
38
39
40
41
42
43
44
45
46
47
48
49
50
51
52
53
54
55
56
57
58
59
60

KEYWORDS. amyloid β-peptide, Alzheimer's disease, peptidomimetics, glycopeptides, aggregation, oligomers, capillary electrophoresis, nuclear magnetic resonance, surface plasmon resonance

ABSTRACT. How anti-Alzheimer's drug candidates that reduce amyloid 1-42 peptide fibrillization interact with the most neurotoxic species is far from being understood. We report herein the capacity of sugar-based peptidomimetics to inhibit both $A\beta_{1-42}$ early oligomerization and fibrillization. A wide range of bio- and physico-chemical techniques, such as a new capillary electrophoresis method, nuclear magnetic resonance, and surface plasmon resonance, were used to identify how these new molecules can delay the aggregation of $A\beta_{1-42}$. We demonstrate that these molecules interact with soluble oligomers in order to maintain the presence of non-toxic monomers and to prevent fibrillization**.** These compounds totally suppress the toxicity of $A\beta_{1-42}$ towards SH-SY5Y neuroblastoma cells, even at sub-stoichiometric concentrations. Furthermore, demonstration that the best molecule combines hydrophobic moieties, hydrogen bond donors and acceptors, ammonium groups and a hydrophilic β-sheet breaker element, provides valuable insight for the future structure-based design of inhibitors of $A\beta_{1-42}$ aggregation.

INTRODUCTION

Protein-protein interactions mediating protein aggregation concern at least 30 different proteins and are associated with more than 20 serious human diseases, including Alzheimer's (AD), Parkinson's disease and type 2 diabetes mellitus. The accumulation of extra- or intracellular

1 2 3 4 5 6 7 8 9 10 11 12 13 14 15 16 17 18 19 20 21 22 23 24 25 26 27 28 29 30 31 32 33 34 35 36 37 38 39 40 41 42 43 44 45 46 47 48 49 50 51 52 53 54 55 56 57 58 59 60

protein deposits, often referred to as amyloid, characterize these protein misfolding diseases. AD, which is the most common form of late-life dementia,[1] is associated with accumulation of intraneuronal neurofibrillary tangles and extracellular 'senile' plaques containing insoluble fibrils composed of 40 or 42-residue amyloid-β peptides ($A\beta_{1-40}$ or $A\beta_{1-42}$).[2] Monomeric Aβ peptides convert into fibrils through a complex nucleation process involving the formation of various aggregated species such as soluble oligomers and protofibrils of increasing size.[3-5] Structural studies have reported that oligomeric and fibrillar species share a β-sheet rich conformation,[6-10] however the structure of the different oligomeric species is far from being understood. Although $A\beta_{1-42}$ is not the most abundant amyloid peptide produced *in vivo*, it is the major constituent of amyloid plaques and is far more aggregative and neurotoxic than $A\beta_{1-40}$.[11,12] Experimental evidence supports the hypothesis that low molecular weight oligomers are primarily responsible for the neurodegeneration observed in AD.[2,11,13-16] However, the role of fibrils should not be neglected, because they have been demonstrated not to be inert species, but are able to generate damaging redox activity and promote the nucleation of toxic oligomers.[17,18] Hence it remains crucial to develop inhibitors that can reduce the prevalence of small transient oligomers and also prevent the formation of fibrils. Numerous compounds have been reported as inhibitors or modulators of $A\beta_{1-42}$ aggregation. The main drawbacks of the described molecules that jeopardize their development as drug candidates are: a lack of binding selectivity leading to a high risk for various side-effects for dyes or polyphenol natural products[19]; poor bioavailability and high propensity to self-aggregate for peptide derivatives[20,21]; and a general lack of information regarding their mechanism of action, and in particular on their effects on toxic oligomers formation.[19-21] To our knowledge, rationally designed small and 'druggable' pseudo-

or non-peptidic aggregation inhibitors have been very scarcely reported.[22,23] Some of us have described retro-inverso peptide inhibitors of both early oligomerization and fibrillization.[22]

We previously reported a novel class of glycopeptide derivatives, based on two hydrophobic dipeptides (Ala-Val and Val-Leu) linked to a hydrophilic D-glucopyranosyl scaffold through aminoalkyl and carboxyethyl linkers in C1 and C6 positions, respectively (compound **1**, Figure 1).[24] These pentapeptide analogs were shown to modulate $A\beta_{1\text{-}40}$ and $A\beta_{1\text{-}42}$ aggregation, as demonstrated by fluorescence Thioflavin-T (ThT) assays and transmission electron microscopy (TEM).[24] The flexible and hydrophilic sugar moiety is believed to act as a β-sheet breaker, playing a major role in preventing the interactions between Aβ species and thus inhibiting the aggregation. The introduction of a carbohydrate in peptides can also have a multifaceted impact on the properties of these molecules, such as modulating the hydrophilicity/hydrophobicity balance and conferring resistance to proteolytic cleavage.[25]

In order to further decrease the number of potential sites for proteolytic attack, we have now introduced peptidomimetics in the upper arm in the C6 position. A wide range of bio- and physico-chemical techniques was then used in order to evaluate the activity of the synthesized small hydrosoluble peptidomimetic compounds on the early oligomerization, fibrillization and toxicity of $A\beta_{1\text{-}42}$ and also to identify the $A\beta_{1\text{-}42}$ species targeted by these molecules.

RESULTS

Design

As we have already demonstrated the superiority of the β configuration of the C1 anomeric carbon in our previously reported glycopeptides,[24b] we decided in a first attempt to evaluate the mixture of α and β anomers, to avoid a difficult separation of the two anomers. Furthermore, as

1
2
3
4
5
6
7
8
9
10
11
12
13
14
15
16
17
18
19
20
21
22
23
24
25
26
27
28
29
30
31
32
33
34
35
36
37
38
39
40
41
42
43
44
45
46
47
48
49
50
51
52
53
54
55
56
57
58
59
60

we have also clearly demonstrated the superiority of the amino propyloxy link relative to the amino ethyloxy link, in the C1 position of the sugar moiety,[24b] we decided to prepare glycopeptidomimetics bearing the amino propyloxy link. For the design of the peptidomimetic strands, we chose to replace the *C*-terminal leucine (Leu5 in compound **1**, Figure 1) by the 5-amino-2-methoxybenzhydrazide unit (compounds **2** and **3**, Figure 1), which is a part of the β-strand mimic ("Hao" unit) reported by Nowick and co-workers.[21,26] The introduction of a 5-amino-2-methoxybenzhydrazide unit into β-strand mimics was shown, by some of us, to be extremely effective in the prevention of protein-protein interactions involving intermolecular β-sheets of HIV-1 protease in order to inhibit its dimerization, while increasing the proteolytic stability of the molecules.[27] In a first generation, the valine residue (Val4 in compound **1**, Figure 1) was kept and linked to the 5-amino-2-methoxybenzhydrazide unit (compound **2**, Figure 1). Next, the valine residue was replaced by a lysine residue, to further provide these molecules with the possibility of engaging in electrostatic interactions with $A\beta_{1-42}$, in order to increase their affinity for $A\beta_{1-42}$ (compound **3**, Figure 1).

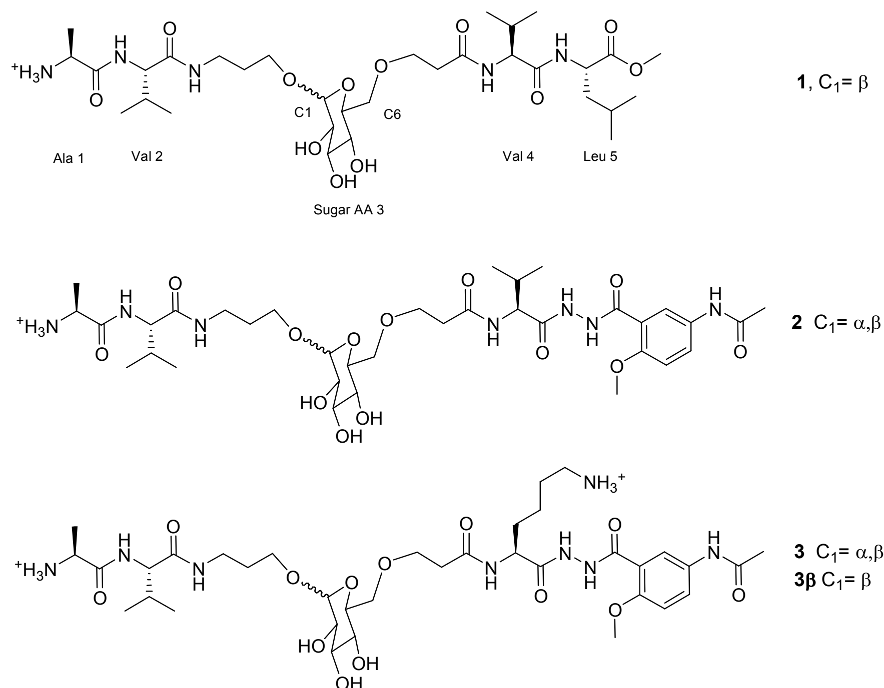

Figure 1. Structure of glycopeptidomimetic derivatives **1**-**3**

Synthesis of the glycopeptidomimetics

A short and robust synthesis of the intermediate **9** was developed (Scheme 1A). We started from the C1 allylic protected D-glucose which was transformed into 4 following the procedure described in the literature.[28] The Michael addition of **4** on tert-butylacrylate was performed to give **5**. The allyl group of **5** was then removed from the C1 hydroxyl group with $PdCl_2$ to give compound **6** in good yield. The anomeric hydroxyl of **6** was converted into the trichloroacetimidate intermediate **7**, in the presence of trichloroacetonitrile and using NaH as a base. The nucleophilic substitution reaction by 3-azidopropan-1-ol was then carried out in the presence of AuCl (10%) affording **8** in good yield. The α and β epimers **8** were obtained in equal proportion and could not be separated at this stage. The tert-butyl group was finally cleaved in acidic conditions to give the carboxylic acid **9**.

1
2
3
4
5
6
7
8
9
10
11
12
13
14
15
16
17
18
19
20
21
22
23
24
25
26
27
28
29
30
31
32
33
34
35
36
37
38
39
40
41
42
43
44
45
46
47
48
49
50
51
52
53
54
55
56
57
58
59
60

The scaffold **9** was then coupled with the peptidomimetic arms **10** and **11** prepared according to our published procedure[27], using DMTMM ([4-(4,6-Dimethoxy1,3,5-triazin-2-yl)-4-methyl-morpholinium tetrafluoroborate])[29] as coupling agent (Scheme 1B). Compounds **12** and **13** were obtained in good yield. The azido group of **12** and **13** was then reduced via a Staudinger reaction[30] to give the corresponding amines, **14** and **15** in satisfactory yields. In order to build the peptidic arm in C1, the two amino acids *N*-Boc-L-Val-OH and *N*-Boc-L-Ala-OH were successively coupled by a standard coupling/deprotection protocol to afford **18** and **19** from **14** and **15** respectively, in good yields. Hydrogenolysis of **18** and **19** afforded **20** and **21**, which underwent an acidic cleavage of the *tert*-butyl carbamate to give **2** and **3**. The acidic cleavage of the *tert*-butyl carbamate was also performed on benzylated compounds **18** and **19** to afford **22** and **23**. All the desired compounds were obtained as a mixture of α and β anomers. The β anomer **3β** was isolated after separation by HPLC.

A

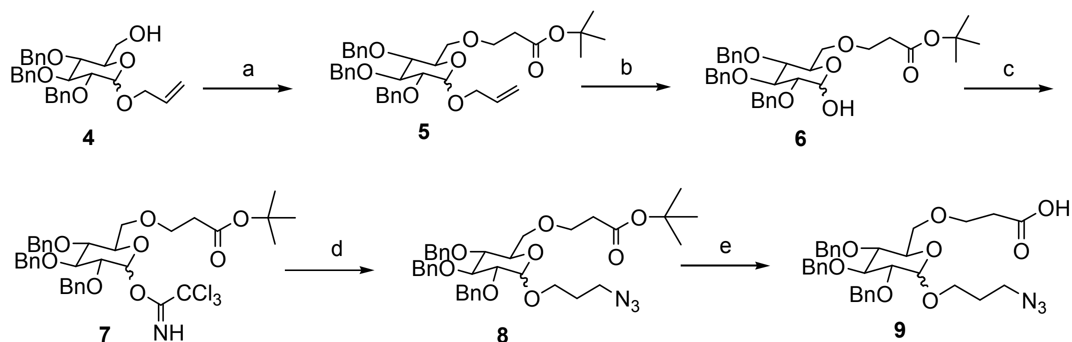

B

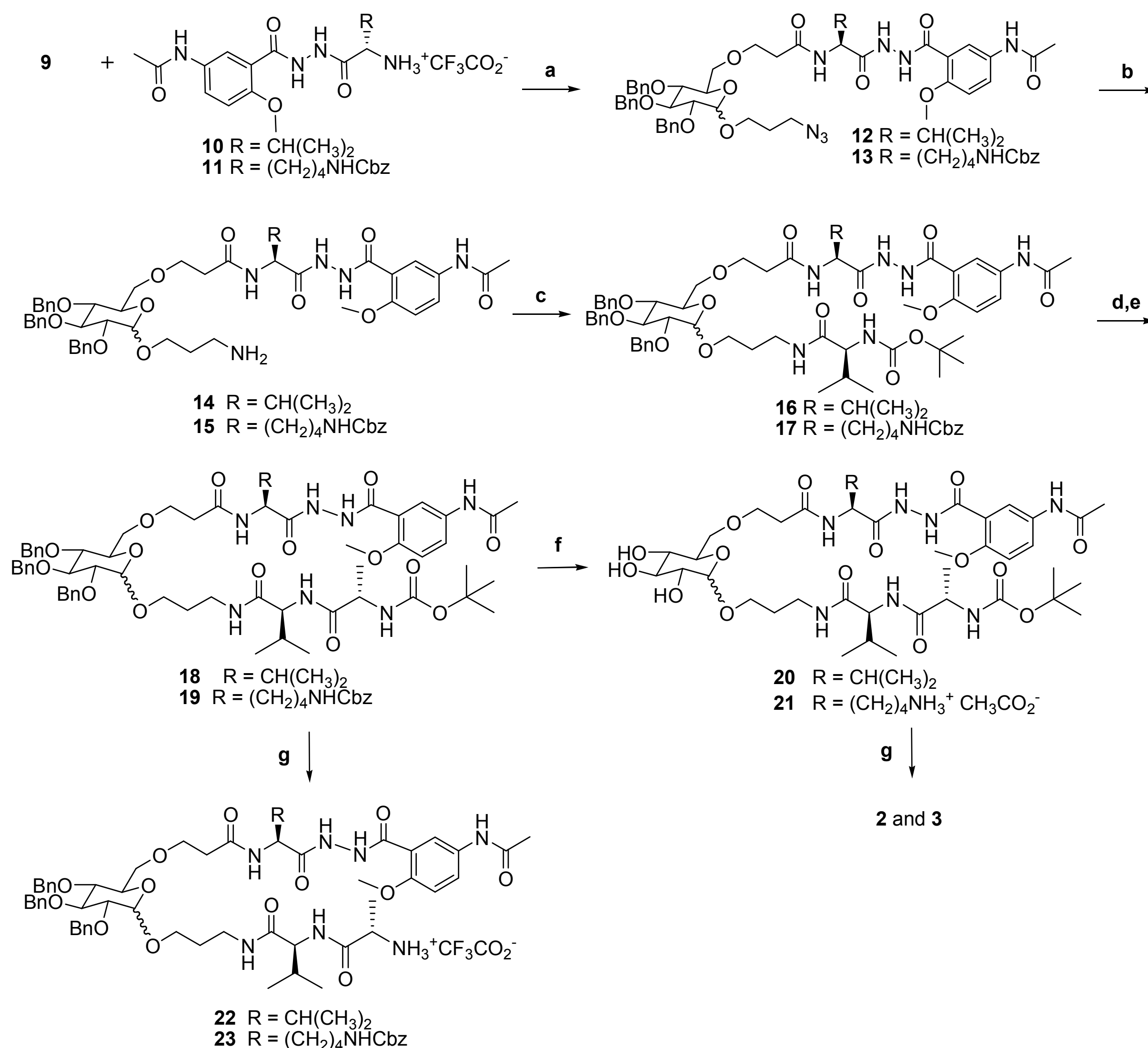

Scheme 1. Synthesis of glycopeptidomimetics. A- Synthesis of the scaffold **9**. Reagents and conditions: a) *tert*-butyl acrylate, TBAB, 20% NaOH aq., rt, 24h, 79%; b) $PdCl_2$, CH_3OH/EtOH, N_2 atm. rt, overnight 75% ; c) CCl_3CN, NaH, CH_2Cl_2, rt, overnight, 75%; d) 3-azidopropan-1-ol, AuCl (10% w/w), CH_2Cl_2, N_2 atm., rt, 2 days, 82%; e) TFA, CH_2Cl_2, rt, overnight, 72%. B- Synthesis of glycopeptidomimetics **2** and **3**. Reagents and conditions: a) NMM, DMTMM, DMF, rt, overnight, 86% (**12**), 68%, (**13**); b) Ph_3P, THF/H_2O (9:1), 40 °C, 24h, 63% (**14**), 50% (**15**); c) *N*-Boc-L-Val-OH, NMM, DMTMM, DMF, rt, overnight, 79% (**16**), 68% (**17**); d) TFA, CH_2Cl_2,

1
2
3
4
5
6
7
8
9
10
11
12
13
14
15
16
17
18
19
20
21
22
23
24
25
26
27
28
29
30
31
32
33
34
35
36
37
38
39
40
41
42
43
44
45
46
47
48
49
50
51
52
53
54
55
56
57
58
59
60

rt, 3h, quantitative; e) *N*-Boc-L-Ala-OH, NMM, DMTMM, rt, overnight, 68% (**18**), 73% (**19**); f) H_2 Pd/C, rt, MeOH, 48h, 88% (**20**); 75% (**21**); g) TFA, CH_2Cl_2, rt, 3h, quantitative.

Inhibition of $A\beta_{1-42}$ fibrillization by glycopeptidomimetics

ThT-fluorescence assays

The ability of compounds **1-3** and of intermediates **19-23** to inhibit the fibrillization of $A\beta_{1-42}$ was studied by ThT fluorescence spectroscopy.[31] The fluorescence curve for $A\beta_{1-42}$ at a concentration of 10 μM followed the typical sigmoidal pattern with a lag phase of 8–9 h followed by an elongation phase and a final plateau reached after 17-18 h (purple curve, Figure 2A). Two parameters were derived from the ThT curves of $A\beta_{1-42}$ alone and $A\beta_{1-42}$ in the presence of the evaluated compound: (1) $t_{1/2,}$ which is defined as the time at which the half maximal ThT fluorescence is observed and gives insight on the rate of the aggregation process; (2) F, the fluorescence intensity at the plateau which is assumed to be dependent on the amount of fibrillar material formed (Table 1, Figures 2A-C).

The glycopeptidomimetic molecules **2** and **3** were dramatically more efficient inhibitors of $A\beta_{1-42}$ aggregation than the glycopeptide compound **1** in particular at lower compound/ $A\beta_{1-42}$ ratios of 1/1 and even 0.1/1. It is noteworthy that a lysine residue attached to the 5-amino-2-methoxybenzhydrazide unit was highly beneficial for the activity compared to a valine residue (compare **3** vs **2** and **21** vs **20**). The free amine of the lysine residue side chain is thus beneficial for the activity. However, no dramatic effect of the *N*-terminal free amine of the dipeptide Val-Ala chain was observed in both lysine and valine series. Indeed, a similar activity was obtained for the free amine **3** and the Boc protected **21** from one hand and for the free amine **2** and the Boc protected **20** on the other hand. It was also remarkable that the β anomer **3β** showed a superior activity to the mixture of α and β anomers in **3** at low compound/$A\beta_{1-42}$ ratios (1/1 and

1
2
3
4
5
6
7
8
9
10
11
12
13
14
15
16
17
18
19
20
21
22
23
24
25
26
27
28
29
30
31
32
33
34
35
36
37
38
39
40
41
42
43
44
45
46
47
48
49
50
51
52
53
54
55
56
57
58
59
60

0.1/1, Table 1 and Figures 2A-C). A supplementary ThT fluorescence assay was performed by first, adding compound **3** after 4 hours, when presumably oligomers are already formed and secondly, adding compound **3** after 42 hours, when presumably essentially fibrils are present (Figure 1S in supporting information). A similar activity was obtained with compound **3** added at the beginning of the kinetics or after 4 hours. However no effect (or even a slightly increase of fluorescence) was observed when compound **3** was added after 42 hours. As also observed in our previous glycopeptides series,[24b] benzylated derivatives **19**, and **22-23** tended to self-aggregate and to slightly accelerate the aggregation process (Table 3S and Figure 1S in supporting information), confirming that polar hydroxyl groups of the sugar moiety were essential to prevent the aggregation.

Table 1. Effects of compounds **1**, **2**, **3**, **3β**, **20** and **21** on $A\beta_{1\text{-}42}$ fibrillization assessed by ThT-fluorescence spectroscopy at a compound/$\mathbf{A\beta_{1\text{-}42}}$ ratio of 10/1 and 1/1 (the concentration of $A\beta_{1\text{-}42}$ in this assay is 10 μM)**.** The effect of **3** and **3β** at a compound/Aβ ratio of 0.1/1 is also reported.

Compounds (Compound/Aβ ratio)	$t_{1/2}$ increase (%) [a]	Plateau decrease (%) [b]
1 10/1	280±70	–56±9
1 1/1	ne	ne
2 10/1	325 ± 12	–31±7
2 1/1	155± 10	ne
3 10/1	NA	–87±1

1
2
3
4
5
6
7
8
9
10
11
12
13
14
15
16
17
18
19
20
21
22
23
24
25
26
27
28
29
30
31
32
33
34
35
36
37
38
39
40
41
42
43
44
45
46
47
48
49
50
51
52
53
54
55
56
57
58
59
60

3 1/1	148±12	–29±9
3 0.1/1	ne	–23±6
3β 10/1	NA	–90±2
3β 1/1	165±11	–34±7
3β 0.1/1	129±12	–16±6
20 10/1	379±15	–41±22
20 1/1	138±10	ne
21 10/1	NA	–84±3
21 1/1	154±8	–26±6

ne = no effect, NA = no aggregation, parameters are expressed as mean ± SE, n=3-6. [a] See supporting information for the calculation of the $t_{1/2}$ increase. A compound displaying a $t_{1/2}$ increase > 100 % is a delayer of aggregation. [b] See supporting information for the calculation of the plateau decrease.

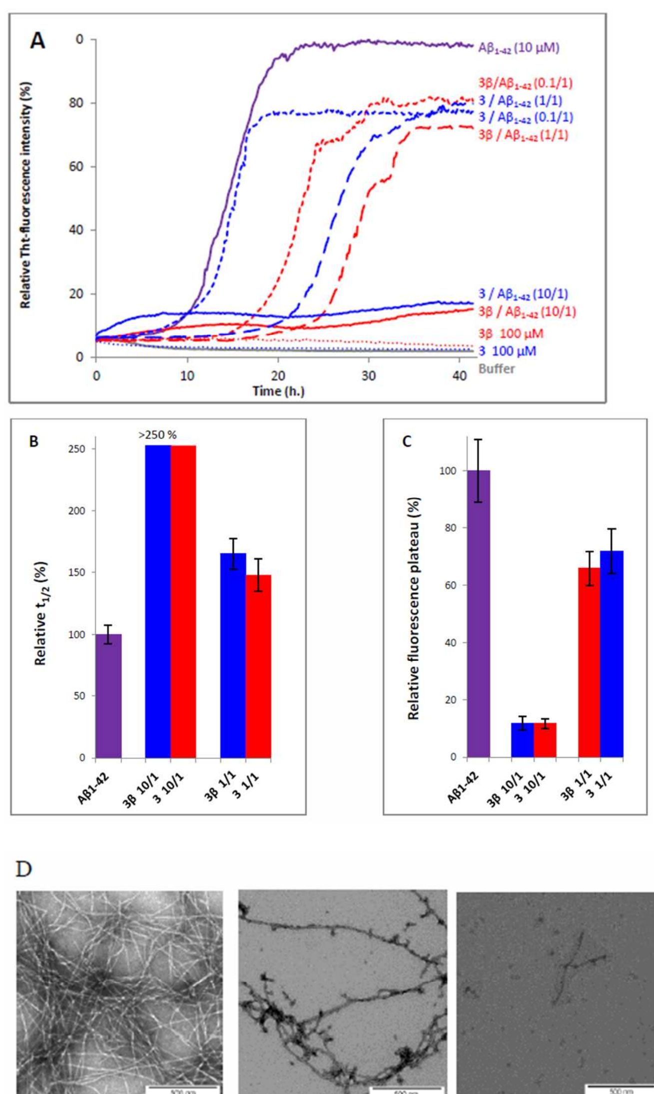

Figure 2. Effects of derivatives **3** and **3β** on the fibrillization kinetics of $A\beta_{1-42}$ monitored by Thioflavin-T fluorescence and TEM. A) Representative curves of ThT fluorescence assays over time showing $A\beta_{1-42}$ (10 µM) aggregation in the absence (purple curve) and in the presence of compounds **3** (blue curves) and **3β** (red curves) at compound/$A\beta_{1-42}$ ratios of 10/1, 1/1 and 0.1/1. B) $t_{1/2}$ increase relative to $A\beta_{1-42}$ alone, in the presence of compounds **3** (blue curves) and **3β** (red curves) at compound/$A\beta_{1-42}$ ratios of 10/1 and 1/1. C) Fluorescence plateau decrease relative to Aβ1-42 alone, in the presence of compounds **3** (blue curves) and **3β** (red curves). D) Effects of derivative **3** on the fibril formation of $A\beta_{1-42}$ visualized by TEM. Negatively stained images were

1
2
3
4
5
6
7
8
9
10
11
12
13
14
15
16
17
18
19
20
21
22
23
24
25
26
27
28
29
30
31
32
33
34
35
36
37
38
39
40
41
42
43
44
45
46
47
48
49
50
51
52
53
54
55
56
57
58
59
60

recorded after 42 h of incubation of $A\beta_{1-42}$ (10 µM in 10 mM Tris.HCl, 100 mM NaCl at pH = 7.4) alone (left) or in the presence of 10 µM of **3** (middle) and of 100 µM of **3** (right). Scale bars, 500 nm.

TEM experiments

Transmission electron microscopy (TEM) analyses were performed on compound **3** that showed a more significant effect than **2** on $A\beta_{1-42}$ aggregation in the ThT-fluorescence assays. Images were recorded after 42 h of preincubation, corresponding to maximum aggregation in the ThT assays, with and without **3** (Figure 2D). Differences were observed regarding the amount of aggregates formed in the presence of **3** at both ratios. A very dense network of fibers displaying a typical morphology was observed for $A\beta_{1-42}$ alone. Only few scattered, very short and scarce fibers were visible on the grid containing the Aβ sample incubated with **3** at 10/1 ratio. This result validated the ThT-fluorescence data, indicating that compound **3** dramatically slowed down the aggregation of $A\beta_{1-42}$ (at **3**/$A\beta_{1-42}$ ratio of 10/1) and efficiently reduced the amount of typical amyloid fibrils formed. It is noteworthy that even if at a **3**/$A\beta_{1-42}$ ratio of 1/1 the fluorescence was not dramatically decreased in the ThT assays, but the morphology of the network observed by TEM was very different and less dense and the sample contained some globular aggregates.

Inhibition of $A\beta_{1-42}$ oligomerization by glycopeptidomimetics

Capillary electrophoresis

In order to determine their effect on small soluble oligomer formation, **3** and **3β** were studied by Capillary Electrophoresis (CE). We recently proposed an improved CE method to monitor easily over time the very early steps of the $A\beta_{1-42}$ oligomerization process.[32,24b] This technique

has the advantage of being able to follow three kinds of soluble species, (i) the monomer (peak ES), (ii) different small metastable oligomers grouped under peak ES' and (iii) transient species formed later and which correspond to species larger than dodecamers (peak LS). Aggregation kinetics of $A\beta_{1-42}$ alone showed that over time, the monomer ES peak decreased in favor of the oligomer peaks ES' and LS, and of insoluble species, forming spikes in the profile (Figure 2S in supporting information for the detailed kinetics). At time 0, the monomer peak ES was almost the only visible species, while after 12 h, only a small monomer peak remained and many insoluble aggregates, giving spikes, were present (Figure 3A).

In the presence of **3β** (**3β** /$A\beta_{1-42}$ ratio of 1/1), the electrophoretic profile clearly indicated that the kinetics of aggregation was significantly slowed down. Indeed, **3β** maintained dramatically the presence of the monomer (peak ES). In addition, the large oligomer species grouped under the peak LS were still present at 12 h while they completely disappeared in the control electrophoretic profile (Figure 3B, and Figure 3S in supporting information for the detailed kinetics). The preservation of the monomer was statistically significant, after 12 h, only 19% remained in the control experiment while 52% remained in the presence of **3β** (Figure 3C). Similar results were observed with the mixture of α and β anomers in **3**, however a slightly superior effect was observed for **3β** (41% of monomer species remained after 12 h in the presence of the mixture **3**) (Figures 4S and 5S in supporting information).

1
2
3
4
5
6
7
8
9
10
11
12
13
14
15
16
17
18
19
20
21
22
23
24
25
26
27
28
29
30
31
32
33
34
35
36
37
38
39
40
41
42
43
44
45
46
47
48
49
50
51
52
53
54
55
56
57
58
59
60

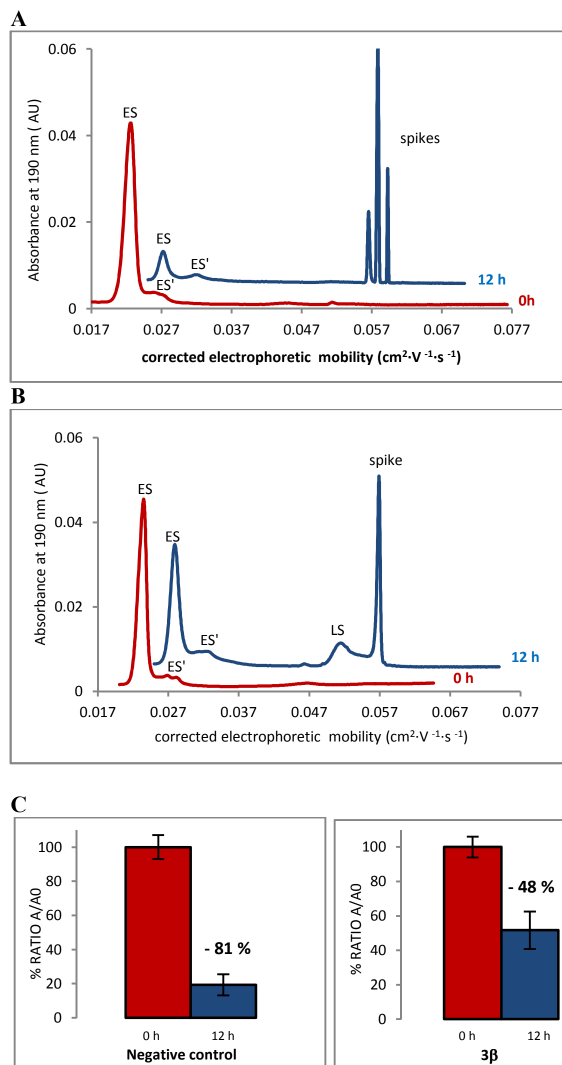

Figure 3. Effect of **3β** on the early oligomerization steps by CE. Electrophoretic profile of **A$\beta_{1\text{-}42}$** peptide (100 µM) obtained immediately (0 h), and 12 h after sample reconstitution (t0) alone (A) and in the presence of compound **3β** at compound/**A$\beta_{1\text{-}42}$** ratio of 1/1 (B). Results in panel show the effect of **3β** on the monomer ES (C). Results are a mean of 3 experiments.

Interaction of 3β with monomeric or oligomeric species of A$\beta_{1\text{-}42}$

NMR experiments

1
2
3
4
5
6
7
8
9
10
11
12
13
14
15
16
17
18
19
20
21
22
23
24
25
26
27
28
29
30
31
32
33
34
35
36
37
38
39
40
41
42
43
44
45
46
47
48
49
50
51
52
53
54
55
56
57
58
59
60

The goal of the NMR experiments was to study if compound **3β** was able to adopt any preferred conformation in solution and if it interacted in solution either with the monomeric species or with soluble aggregated forms of $Aβ_{1-42}$.

We first examined mixtures of $Aβ_{1-42}$ and **3β** at a temperature of 5°C and using low concentrations of $Aβ_{1-42}$ (10–90 μM) to ensure that $Aβ_{1-42}$ was mainly monomeric in freshly prepared samples.[33] The 2D ^{1}H-^{15}N and 2D ^{1}H-^{13}C HSQC spectra of 10 μM ^{15}N,^{13}C-labelled $Aβ_{1-42}$[34] recorded in the absence and in the presence of a large excess of 3β (0.4 mM) displayed no significant chemical shift perturbations of $Aβ_{1-42}$ ^{1}H-^{15}N and ^{1}H-^{13}C correlations (Figure 6S in supporting information). Similarly, no chemical shift differences could be detected for the ^{1}H signals of **3β** in 1D ^{1}H and 2D ^{1}H-^{1}H experiments (data not shown), even when higher concentrations of $Aβ_{1-42}$ were used (up to 90 μM). Thus NMR experiments demonstrated that **3β** did not interact with monomeric $Aβ_{1-42}$ peptide.

We then turned to magnetization transfer experiments that are commonly used to detect the binding of small ligands to large molecular weight species. Saturation Transfer Difference (STD) experiments were recorded to characterize binding properties and map binding epitopes of **3β**.[24a, 35] No STD signals could be detected in a control experiment with **3β** alone, as expected for a low molecular weight molecule that did not aggregate in solution. The addition of $Aβ_{1-42}$ peptide led to the apparition of weak STD signals (Figure 4). Interestingly, an increase in the STD signal was observed over time, reaching a maximum after 2.5 weeks. Concomitantly, a slow decay of the 1D ^{1}H NMR signals of $Aβ_{1-42}$ was observed (Figure 7S in supporting information), corresponding to the formation of high molecular weight $Aβ_{1-42}$ aggregates that were too large to be observed by solution NMR spectroscopy.[33] Thus the gradual increase of the STD signal over several weeks could be explained by the slow conversion of monomeric $Aβ_{1-42}$ to aggregated

1
2
3
4
5
6
7
8
9
10
11
12
13
14
15
16
17
18
19
20
21
22
23
24
25
26
27
28
29
30
31
32
33
34
35
36
37
38
39
40
41
42
43
44
45
46
47
48
49
50
51
52
53
54
55
56
57
58
59
60

species that bind **3β**. The STD signals were the strongest for the aromatic and methyl resonances of **3β**, suggesting that the hydrophobic groups of the dipeptide and peptidomimetic strands were directly involved in the interaction with $A\beta_{1-42}$ species.

WaterLOGSY experiments also enabled us to detect the binding of **3β** to $A\beta_{1-42}$ species, through intermolecular magnetization transfers involving bulk water. The protons of **3β** exhibited positive NOEs in the absence of $A\beta_{1-42}$ (Figure 8S in supporting information), as expected for a small molecule. The addition of $A\beta_{1-42}$ caused a decrease of positive NOEs and a change of sign of the NOEs that became more negative over time, confirming that **3β** binds to high molecular weight species in fast exchange on the NMR time scale.

Finally, NMR spectroscopy was used to analyze the structure of **3β** in the free and bound forms. The 1D ^{1}H NMR spectra of **3β** alone were characterized by sharp line widths and concentration-independent chemical shifts (0.04–2 mM range), demonstrating that **3β** was highly soluble and not prone to aggregation in the (sub) millimolar range. Chemical shifts, vicinal coupling constants and ROEs analysis showed that the peptidic/pseudopeptidic arms and the aminoalkyl and carboxyethyl linkers were highly flexible, as supported by small diastereotopic splitting of methylenic protons, averaged vicinal coupling constants (Table S1 in supporting information), intraresidual and sequential ROE intensities, and the absence of long-range ROEs. Furthermore the amide protons exhibited strong temperature dependence of their chemical shifts (Table S1 in supporting information), which is an indicator of high solvent accessibility. Altogether, these NMR data indicated that **3β** did not adopt *per se* hydrogen-bonded β-sheet conformations and had no self-association properties in solution. Interestingly, 2D NOESY experiments recorded on **3β** in the presence of $A\beta_{1-42}$ were characterized by modifications in the intensity of intraresidual and sequential NOEs which became more negative (Figure 9S in

supporting information). These changes correspond to transferred NOEs due to transient binding of **3β** to A$β_{1-42}$ aggregated species. However no additional long-range NOE correlations were detected, suggesting that **3β** conformation remained largely extended and did not adopt a compact shape upon A$β_{1-42}$ binding.

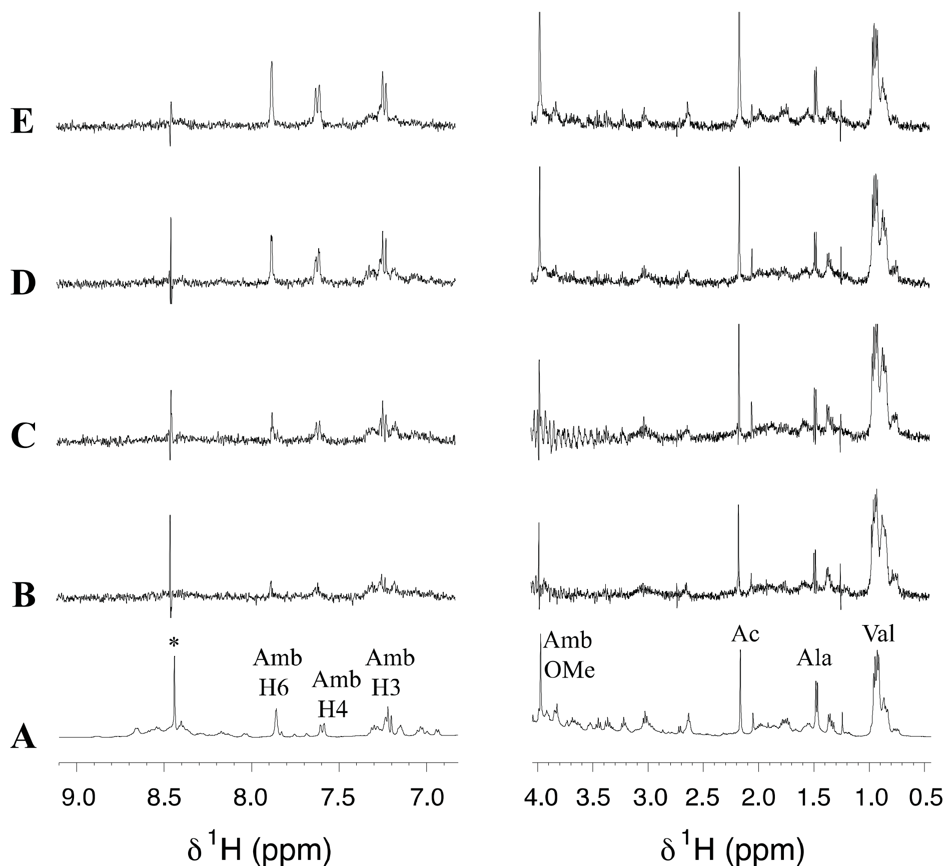

Figure 4. Interaction of **3β** with A$β_{1-42}$ monitored by NMR. Aromatic/amide (left) and aliphatic (right) regions of 1D ^{1}H NMR spectra of **3β** (0.4 mM) and A$β_{1-42}$ (90 μM) at 5°C. (A) Reference 1D ^{1}H spectrum recorded at t = 0. (B-E) 1D ^{1}H STD spectra recorded at t = 0 (B), after 2 days (C), 1 week (D) and 2.5 weeks (E). The assignment of the aromatic and methyl resonances of **3β** is indicated. Amb means 5-amino-2-methoxybenzoyl. The signal marked with an asterisk corresponds to formic acid impurity.

1 2 3 4 5 6 7 8 9 10 11 12 13 14 15 16 17 18 19 20 21 22 23 24 25 26 27 28 29 30 31 32 33 34 35 36 37 38 39 40 41 42 43 44 45 46 47 48 49 50 51 52 53 54 55 56 57 58 59 60

SPR experiments

SPR was then used to evaluate the affinity between compound **3** and its β-anomer **3β** and $A\beta_{1-42}$ monomer bound to the gold surface.

To our knowledge, the few SPR experiments described in the literature to detect the affinity of ligands for $A\beta_{1-42}$ have used either the depsi-peptide molecule described by Taniguchi et al.[36,37,22] or biotinylated $A\beta_{1-42}$ immobilized onto streptavidin-coated chips.[38] An SPR-based immunoassay has been also developed to recognize $A\beta_{1-42}$ oligomers.[39] The main drawbacks we found in these methods are the necessity to synthesize the non-commercial depsi-peptide, the modest SPR response provided with these other approaches, and the use of modified peptides which may alter their affinity behavior. We thus developed a new method to immobilize the commercial $A\beta_{1-42}$ peptide monomer by a classical peptide coupling through its amino groups. We paid particular attention to maintaining $A\beta_{1-42}$ in its monomeric form upon immobilization. Recently a similar method has been reported, however no clear evidence on the nature of the immobilized species was provided.[40]

We optimized the immobilization of $A\beta_{1-42}$ peptide by varying different parameters (pH and concentration of the sample preparation, and injection parameters such as the flow, the time and the number of injections). To ensure that only monomeric species were mainly immobilized, a rinsing step using an aqueous solution of $NH_4OH.H_2O$ 0.1 % was employed (see the procedure in supporting information), as we demonstrated previously by CE that these conditions were able to disaggregate oligomers and regenerate monomeric species.[32] The characterization of the gold chip was performed using specific antibodies directed against the *N*- or *C*-term of $A\beta_{1-42}$ (6E10 and MD 19-0016, respectively, see supporting information). Curcumin, which is a well-known disaggregant compound[41] did not lead to a decrease of the signal and was even found to bind to

1
2
3
4
5
6
7
8
9
10
11
12
13
14
15
16
17
18
19
20
21
22
23
24
25
26
27
28
29
30
31
32
33
34
35
36
37
38
39
40
41
42
43
44
45
46
47
48
49
50
51
52
53
54
55
56
57
58
59
60

$A\beta_{1-42}$ fixed on the SPR chips (Figure 18S in supporting information). Finally, the affinity of ThT toward the peptide immobilized on the chip surface was evaluated before and after our optimized rinsing step, which used an aqueous solution of $NH_4OH.H_2O$ 0.1 %. Both SPR signal and fluorescence (visualized by fluorescence microscopy images of the channel) were higher before the rinsing step. The rinsing step is therefore crucial to disaggregate large species present initially on the chip surface in order to lead to a surface mainly composed by Aβ in its monomeric form (Figure 14S in supporting information).

We conducted SPR measurements with compounds **3**, **3β** and **1** to check their affinity for $A\beta_{1-42}$ peptide. A concentration-dependent signal was observed, however, the response was very low in the range of the tested concentrations (up to 200 μM) indicating that these compounds have a very low affinity for the immobilized $A\beta_{1-42}$ (Figures 15S, 16S and 17S in supporting information). This result is in accordance with the NMR data.

Protection against $A\beta_{1-42}$ cell toxicity

The inhibitors were investigated to determine their ability to reduce the toxicity of aggregated $A\beta_{1-42}$ to SH-SY5Y neuroblastoma cells. The addition of either **1** or **3** showed a protective effect on cell survival (MTS assay, Figure 5) and membrane damage (LDH membrane integrity assay, Figure 19S in supporting information) in the presence of cytotoxic 5 μM $A\beta_{1-42}$. Remarkably, this protective effect was seen at equimolar amounts of inhibitor to $A\beta_{1-42}$ and was still significant at a very low ratio of 0.1/1 (inhibitor/$A\beta_{1-42}$) in the MTS assay.

1
2
3
4
5
6
7
8
9
10
11
12
13
14
15
16
17
18
19
20
21
22
23
24
25
26
27
28
29
30
31
32
33
34
35
36
37
38
39
40
41
42
43
44
45
46
47
48
49
50
51
52
53
54
55
56
57
58
59
60

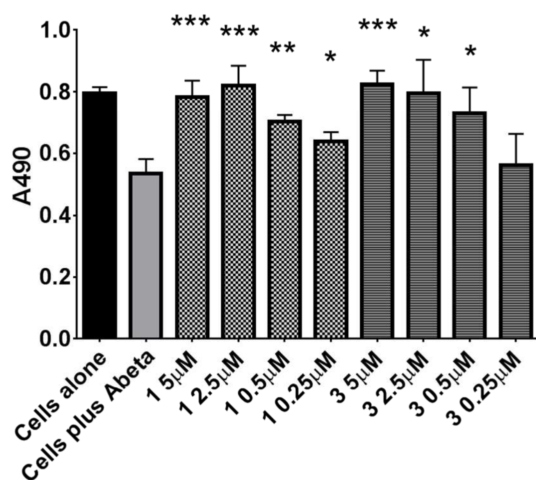

Figure 5. Effect of **1** and **3** on Aβ_{1-42} toxicity towards SH-SY5Y cells. Cell viability in the presence of 5 μM aggregated **Aβ_{1-42}** and decreasing concentrations of **1** or **3**. The black bar on the left shows cell viability in the absence of Aβ_{1-42}. Statistical significance is indicated by *, where * is $p<0.05$, ** is $p<0.01$ and *** is $p<0.001$ comparing cells incubated with **Aβ_{1-42}** plus inhibitor to those with **Aβ_{1-42}** alone. Statistical significance is described.

Plasma stability

The ability to withstand enzymatic cleavage in the circulatory system is an important requirement for any potential drug. Incubating the two inhibitors **1** and **3** in plasma gives an idea of how stable they will be once injected into the body. **3** withstood 24 hours at 37˚C with no obvious degradation in 10% plasma (Figure 20S in supporting information). **1** appeared to show some degradation over the same period, although the total area of the peaks did not change (Figure 20S in supporting information). Unmodified polypeptides are usually degraded within minutes under these incubation conditions.

1
2
3
4
5
6
7
8
9
10
11
12
13
14
15
16
17
18
19
20
21
22
23
24
25
26
27
28
29
30
31
32
33
34
35
36
37
38
39
40
41
42
43
44
45
46
47
48
49
50
51
52
53
54
55
56
57
58
59
60

DISCUSSION

The introduction of a peptidomimetic strand based on a 5-amino-2-methoxybenzhydrazide unit linked through the carboxyethyl in the C6 position of the D-glucopyranosyl scaffold not only increased the stability towards proteolytic degradation but also dramatically increased the capacity of these pentapeptide analogs to inhibit the fibrillization of $A\beta_{1-42}$, as demonstrated by the ThT fluorescence and TEM experiments. The polar hydroxyl groups of the sugar moiety were essential to prevent the aggregation, as demonstrated by the lack of inhibitory activity of the benzyl analogues **19**, **22-23**. A slightly superior effect was observed for the β anomer **3β** compared to the mixture of α and β anomers in **3** (confirmed in the CE experiments). The presence of the amine of the side chain of the lysine residue in compound **3** proved to be beneficial for the inhibitory activity in comparison with the valine residue in compound **2**. This result suggests that an ionic interaction is likely to be established between this amine and acidic residues of $A\beta_{1-42}$, strengthening the hydrophobic interactions involving aliphatic and aromatic moities. Indeed, several computational and experimental studies on $A\beta_{1-42}$ have shown that, in addition to the hydrophobic interactions involving in particular the 16-21 sequence (KLVFFA), the formation of a salt-bridge between amino acids Asp23 and Lys28 might stabilize a turn motif involving residues 24-28.[9,42] An interaction with Glu22 might also be beneficial for the activity of the molecules.[42b] We can thus suggest, and this is supported by the NMR binding experiments (STD), that this novel class of glycopeptidomimetics is likely to interact through the hydrophobic sequences of the peptidomimetic and dipeptide sequences, presumably with a hydrophobic sequence of $A\beta_{1-42}$ (such as the central K_{16}-A_{21} or the C-terminal part I_{31}-V_{40}) and through an electrostatic interaction. The flexible and hydrophilic sugar moiety acts as a β-sheet breaker to prevent the aggregation. The effect of the glycopeptidomimetic on the early steps of

1
2
3
4
5
6
7
8
9
10
11
12
13
14
15
16
17
18
19
20
21
22
23
24
25
26
27
28
29
30
31
32
33
34
35
36
37
38
39
40
41
42
43
44
45
46
47
48
49
50
51
52
53
54
55
56
57
58
59
60

oligomerization has been also demonstrated clearly by CE. Compound **3β** dramatically preserved the non-toxic monomer of $A\beta_{1-42}$ (ES). Oligomers larger than dodecamers (LS) were also stabilized. Both types of cell viability assay proved that pre-incubation of cytotoxic $A\beta_{1-42}$ with glycopeptidomimetic **3** completely rescued the SH-SY5Y neuroblastoma cells. The protective effect was observed even at sub-stoichiometric concentrations (**3** reduced cell death by 100% with 0.5 eq and by 75% with 0.1 eq. in the MTS assay). This protective effect is much more pronounced than that observed with molecules which have undergone clinical trials, such as resveratrol[43], scyllo-inositol[44], epigallocatechin-3-gallate (EGCG)[44,45] or other molecules recently described as efficient reducers of $A\beta_{1-42}$ toxicity.[46] This effect is comparable to the best effect of the current Aβ aggregation inhibitors reported in the literature.[22] Indeed, these molecules reduced $A\beta_{1-42}$ toxicity only at stoichiometric or higher (5 to 10 equivalents) concentrations. It is also noteworthy that glycopeptide **1** showed a dramatic effect on cell survival, but was more sensitive to proteolytic attack.

The NMR and SPR experiments clearly indicated that this novel glycopeptidomimetic series does not bind to monomers with substantial affinity. NMR indicated that the $A\beta_{1-42}$ species recognized by **3β** are oligomeric forms whose concentration slowly increased with time. Thus, even if **3β** is a small molecule that does not per se adopt a preferential conformation, it is able to recognize and bind to the early β-structured $A\beta_{1-42}$ oligomers. The observation of magnetization transfers in STD, WaterLOGSY and trNOESY experiments implied that the interconversion between the free and the $A\beta_{1-42}$-bound forms of **3β** occurred in fast exchange on the NMR time scale. We can thus hypothesize that such transient binding of **3β** to oligomers may impede the subsequent addition of monomers or the association of oligomers into larger species and/or disrupt these early oligomers so that they revert back to monomers (Figure 6A).

1
2
3
4
5
6
7
8
9
10
11
12
13
14
15
16
17
18
19
20
21
22
23
24
25
26
27
28
29
30
31
32
33
34
35
36
37
38
39
40
41
42
43
44
45
46
47
48
49
50
51
52
53
54
55
56
57
58
59
60

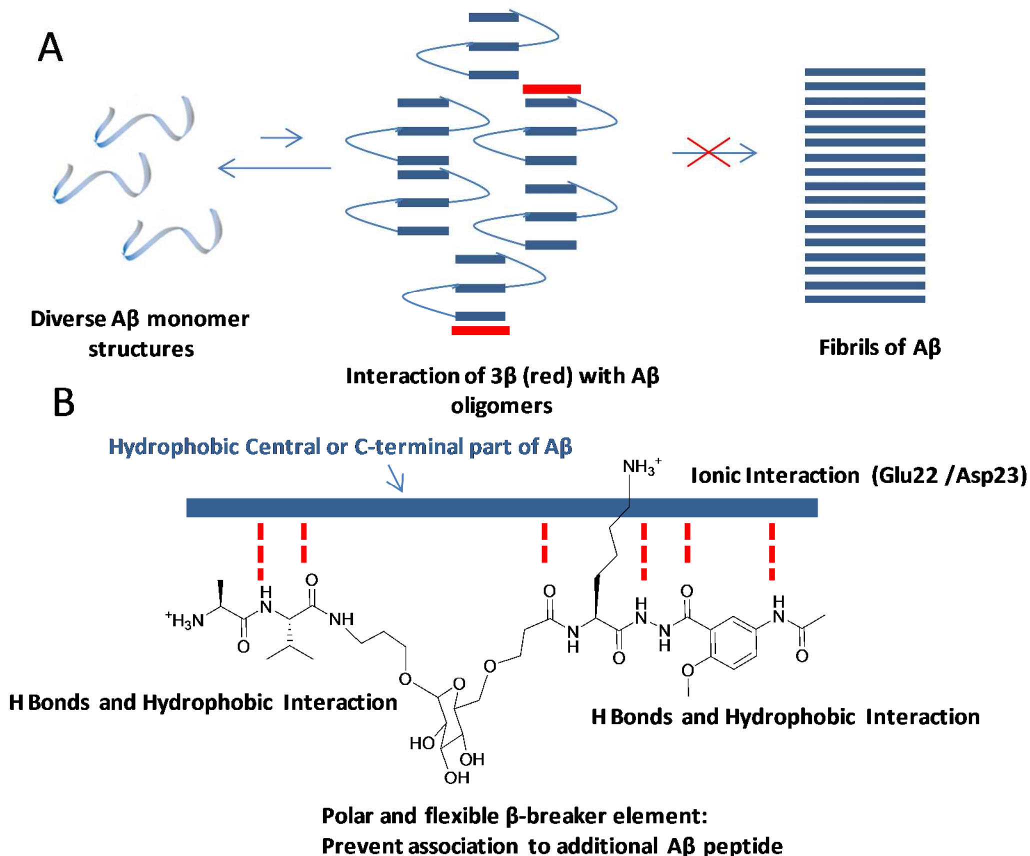

Figure 6. Hypothesis of mechanism of $A\beta_{1-42}$ aggregation inhibition by **3β**. A- Proposed model of inhibition of fibrillization of $A\beta_{1-42}$ and of preservation of $A\beta_{1-42}$ monomer by **3β**. B- Proposed model of interaction of **3β** with $A\beta_{1-42}$.

Noteworthy, this inhibition effect is sequence-specific since compound **3** does not alter the kinetics of aggregation of another amyloid peptide, IAPP, involved in type 2 diabetes mellitus. Indeed, the peptidomimetic **3** does not inhibit the IAPP fibril formation even at a high peptidomimetic/ IAPP ratio of 10/1 (see supporting information). The $t_{1/2}$ is not increased after addition of **3** and the final fluorescence intensity remains the same.

1
2
3
4
5
6
7
8
9
10
11
12
13
14
15
16
17
18
19
20
21
22
23
24
25
26
27
28
29
30
31
32
33
34
35
36
37
38
39
40
41
42
43
44
45
46
47
48
49
50
51
52
53
54
55
56
57
58
59
60

CONCLUSION

In conclusion, the present work validates the singular effect of sugar-based peptidomimetic analogs of pentapeptides on $A\beta_{1-42}$ oligomerization and fibrillization. This new series has been designed in order to achieve three objectives: first, to engage hydrophobic, hydrogen bonds and ionic interactions with $A\beta_{1-42}$, thanks to small peptide and peptidomimetic arms; secondly, to prevent cross β-sheet elongation of $A\beta_{1-42}$ due to the hydrophilic sugar, considered as a β-sheet breaker element (Figure 6B). Finally, it has been designed also to be druggable, particularly to be a small molecule (MW around 800) with a good hydrophobicity/ hydrophilicity balance and resistance to proteolytic degradation. A wide range of bio- and physico-chemical techniques was used to demonstrate the capacity of the compounds (in particular **3β**) to delay both the early oligomerization and fibrillization of $A\beta_{1-42}$. To the best of our knowledge, this is the first example of a small molecule being able to preserve the non-toxic monomeric species of $A\beta_{1-42}$, as demonstrated by capillary electrophoresis. The strong protective effect on cells, even at sub-stoichiometric concentrations, also highlights the considerable therapeutic potential of this novel series of peptidomimetics. This protective effect is significantly better that the one observed with molecules which have undergone clinical trials. The structural elements demonstrated here as crucial for the inhibitory activity, i.e. hydrophobic moieties, hydrogen bond donors and acceptors, ammonium groups and hydrophilic β-sheet breakers provide valuable insights to explore also the design of compounds targeting other types of amyloid-forming proteins.

EXPERIMENTAL SECTION

Chemistry

1
2
3
4
5
6
7
8
9
10
11
12
13
14
15
16
17
18
19
20
21
22
23
24
25
26
27
28
29
30
31
32
33
34
35
36
37
38
39
40
41
42
43
44
45
46
47
48
49
50
51
52
53
54
55
56
57
58
59
60

General Experimental Methods. Usual solvents were purchased from commercial sources and dried and distilled by standard procedures. Compounds **4**,[29] **10**[27] and **11**[27] were prepared according to published methods. Pure products were obtained after liquid chromatography using Merck silica gel 60 (40-63 μm). TLC analyses were performed on silica gel 60 F_{250} (0.26 mm thickness) plates. The plates were visualized with UV light (λ = 254 nm) or revealed with a 4 % solution of phosphomolybdic acid in EtOH. Melting points were determined on a Kofler melting point apparatus. Element analyses (C, H, N) were performed on a Perkin-Elmer CHN, Analyser 2400 at the Microanalyses Service of the Faculty of Pharmacy at Châtenay-Malabry (BioCIS, France). NMR spectra were recorded on an ultrafield Bruker AVANCE 300 (^{1}H, 300 MHz, ^{13}C, 75 MHz) or on a Bruker AVANCE 400 (^{1}H, 400 MHz, ^{13}C, 100 MHz). Chemical shifts δ are in ppm and the following abbreviations are used: singlet (s), doublet (d), doublet of doublet (dd), triplet (t), quintuplet (qt), multiplet (m), broad multiplet (bm), and broad singlet (bs). Mass spectra were obtained using a Bruker Esquire electrospray ionization apparatus. HRMS were obtained using a TOF LCT Premier apparatus (Waters), with an electrospray ionization source. The purity of compounds **2**, **19-23** was determined by HPLC using the 1260 Infinity system (Agilent Technologies) and a column SUNFIRE (C18, 3.5 μm, 100 mm X 2.1 mm); mobile phase : MeOH / H_2O + 0.1 % formic acid from 5 to 100 % in 20 min. ; detection at 254 nm ; flow rate 0.25 mL/min. The purity of compounds **3** and **3β** was determined by HPLC using the 1260 Infinity system (Agilent Technologies) and a column SUNFIRE (C18, 5 μm, 150 mm X 2.1 mm); mobile phase for 3 : acetonitrile / H_2O + 0.2 % formic acid from 1 to 100 % in 20 min. ; mobile phase for **3β**: acetonitrile / H_2O + 0.2 % formic acid at ratio 1/99 during 3 min., then gradient to 30/70 in 12 min.; detection at 310 nm ; flow rate 0.25 mL/min.

1
2
3
4
5
6
7
8
9
10
11
12
13
14
15
16
17
18
19
20
21
22
23
24
25
26
27
28
29
30
31
32
33
34
35
36
37
38
39
40
41
42
43
44
45
46
47
48
49
50
51
52
53
54
55
56
57
58
59
60

(2*S*)-*N*-[3-[(3*S*,4*S*,5*S*)-6-[[3-[[(1*S*)-1-[[(5-Acetamido-2-methoxy-benzoyl)amino]carbamoyl]-2-methyl-propyl]amino]-3-oxo-propoxy]methyl]-3,4,5-trihydroxy-tetrahydropyran-2-yl]oxypropyl]-2-[[(2S)-2-aminopropanoyl]amino]-3-methyl-butanamide (2). Same procedure as described for 16a from 20 (35 mg, 0.036 mmol) in dry CH_2Cl_2 (300 µL) to yield **2** (38 mg, quantitative, α/β 60/40) as a white solid. R_f = 0 (CH_2Cl_2/ CH_3OH : 95/5) ; ^{1}H NMR (300 MHz, CD_3OD) : δ = 7.88 (d, *J* = 2.7 Hz, 1H); 7.53 (dd, *J* = 9.0, 2.7 Hz, 1H); 6.90 (d, *J* = 9.0 Hz, 1H); 4.54 (d, *J* = 3.6 Hz, 0.60H, $H_{1\beta}$); 4.19 (d, *J* = 7.0 Hz, 1H,); 4.05 (d, *J* = 7.8 Hz, 0.40H, $H_{1\alpha}$); 3.96 (dd, *J* = 7.7, 2.7 Hz, 1H); 3.86 (m, 1H); 3.76 (s, 3H); 3.64 – 2.96 (m, 12H); 2.36 (m, 2H); 1.96 (m, 1H); 1.91 (s, 3H); 1.81 (m, 1H); 1.58 (m, 2H); 1.29 (d, *J* = 7.0 Hz, 3H); 0.84 (m, 6H); 0.74 (d, *J* = 6.7 Hz, 6H) ; ^{13}C NMR (75 MHz, CD_3OD) : δ = 174.2, 174.1, 173.0, 171.6, 171.0, 165.5, 155.6, 133.3, 126.8, 124.3, 120.9, 113.4, 104.3 ($C_{1H\alpha}$), 100.2 ($C_{1H\beta}$), 77.9, 76.6, 75.0, 73.4, 72.5, 71.6, 71.1, 68.5, 68.4, 67.1, 60.7, 58.7, 57.0, 50.1, 37.8, 37.6, 37.3 (C_8), 31.9, 30.0, 23.7, 19.7, 18.7, 17.7; HRMS (TOF, ESI, ion polarity positive, H_2O/ MeOH): m/z $[M+H]^+$, calcd for $C_{35}H_{58}N_7O_{13}$ 784.4093; found 784.4094, m/z $[M+Na]^+$, calcd for $C_{35}H_{57}N_7O_{13}Na$ 806.3917; found 806.3912; HPLC purity: TR (α, β) = 10.91 min., 95 %.

(2*S*)-*N*-[3-[(3*S*,4*S*,5*S*)-6-[[3-[[(1*S*)-1-[[(5-Acetamido-2-methoxy-benzoyl)amino]carbamoyl]-5-amino-pentyl]amino]-3-oxo-propoxy]methyl]-3,4,5-trihydroxy-tetrahydropyran-2-yl]oxypropyl]-2-[[(2S)-2-aminopropanoyl]amino]-3-methyl-butanamide (3). Same procedure as described for **16a** from **21** (38 mg, 0.040 mmol) in dry CH_2Cl_2 (300 µL) to afford **3** (40 mg, quantitative, α/β 50/50) as a white solid. R_f = 0 (CH_2Cl_2/ CH_3OH : 95/5); ^{1}H NMR (300 MHz, CD_3OD) : δ = 8.16 (sl, 1H); 7.70 (m, 1H); 7.14 (d, *J* = 9.0 Hz, 1H); 4.75 (m, 0.50H, $H_{1\beta}$); 4.54 (m, 1H); 4.26 (d, *J* = 7.8 Hz, 0.50H, $H_{1\alpha}$); 4.14 (m, 1H); 4.02 (d, *J* = 7.1 Hz, 1H); 3.98 (s, 3H); 3.90 (m, 1H); 3.79 (m, 3H); 3.70 (m, 1H); 3.62 (m, 2H); 3.35

1
2
3
4
5
6
7
8
9
10
11
12
13
14
15
16
17
18
19
20
21
22
23
24
25
26
27
28
29
30
31
32
33
34
35
36
37
38
39
40
41
42
43
44
45
46
47
48
49
50
51
52
53
54
55
56
57
58
59
60

(m, 4.6H); 3.16 (m, 0.6H); 3.04 (m, 1H); 2.98 (m, 1H); 2.55 (sl, 2H); 2.12 (s, 3H); 2.03 (m, 1H); 1.90 (m, 2H); 1.77 (m, 4H); 1.57 (m, 2H); 1.50 (d, *J* = 7.1 Hz, 3H); 1.34 (d, *J* = 6.5 Hz, 4H); 0.97 (d, J = 6.5 Hz, 6H) ; ^{13}C NMR (125 MHz, H_2O:D_2O 90:10) : δ = 177.5, 177.1, 175.9, 175.6, 173.6, 169.5, 169.2, 165.6, 158.1, 132.8, 131.5, 131.4, 130.18, 127.8, 121.4, ,121.2, 120.1, 117.8, 115.6, 104.9 ($C_{1H\alpha}$), 103.0, 100.9 ($C_{1H\beta}$), 78.3, 77.3, 75.8, 73.1, 72.4, 72.1, 71.5, 70.3, 69.9, 69.8, 68.1, 63.1, 58.8, 55.6, 55.27, 53.5, 51.6, 47.3, 42.1, 42.0, 39.2, 39.0, 38.5, 38.3, 34.1, 33.2, 33.1, 32.6, 31.1, 31.0, 29.2, 29.1, 28.2, 25.3, 24.9, 24.7, 21.1, 21.0, 20.8, 19.5 ; HRMS (TOF, ESI, ion polarity positive, H_2O/ MeOH): m/z $[M+H]^+$, calcd for $C_{36}H_{61}N_8O_{13}$ 813.4358; found 813.4363; HPLC purity: TR (α, β) = 11.70 min., 100 %.

(2*S*)-N-[3-[(2*R*,3*S*,4*S*,5*S*)-6-[[3-[[(1*S*)-1-[[(5-Acetamido-2-methoxy-benzoyl)amino]carbamoyl]-5-amino-pentyl]amino]-3-oxo-propoxy]methyl]-3,4,5-trihydroxy-tetrahydropyran-2-yl]oxypropyl]-2-[[(2S)-2-aminopropanoyl]amino]-3-methyl-butanamide (3β). Isolation of β anomer **3β** from **3** was performed by HPLC using a WATERS gradient system pump (DELTAPREP, UV detector PDA 2996) and a column sunfire (C18, 5 µm, 150 mm x 19 mm); mobile phase: acetonitrile /H_2O + 0.2 % formic acid at ratio 1/99 during 3 min., then at ratio 60/40 in 12 min. ; flow rate 17 mL/min. ; detection at 310 nm. HRMS (TOF, ESI, ion polarity positive, H_2O/ MeOH): m/z $[M+H]^+$, calcd for $C_{36}H_{61}N_8O_{13}$ 813.4358; found 813.4356 ; HPLC purity: TR = 10.12 min., 100 %. ^{1}H and ^{13}C NMR assignments are shown in supporting information (Tables S1 and S2)

tert-Butyl 3-[(6-allyloxy-3,4,5-tribenzyloxy-tetrahydropyran-2-yl)methoxy]propanoate (5). To a suspension of **4** (7.00 g, 14.27 mmol) in *tert*-butyl-acrylate (4.14 mL, 28.54 mmol) was added TBAB (690 mg, 2.14 mmol) and an aqueous solution of NaOH 20% (60 mL). The reaction mixture, which appeared like an emulsion, was stirred for 24 h at room temperature. At

1
2
3
4
5
6
7
8
9
10
11
12
13
14
15
16
17
18
19
20
21
22
23
24
25
26
27
28
29
30
31
32
33
34
35
36
37
38
39
40
41
42
43
44
45
46
47
48
49
50
51
52
53
54
55
56
57
58
59
60

the end of the reaction, a mixture of EtOAc/H_2O 1/1 (200 mL) was added and the aqueous phase was extracted with EtOAc (3 x 60 mL). The combined organic layers were dried over Na_2SO_4, filtered and concentrated under reduced pressure to give a crude oil which was purified by column chromatography on silica gel with eluent cyclohexane/EtOAc 80/20 to afford **5** as a colourless oil (7.1 g, 79%, α/β 70/30). R_f = 0.45 (cyclohexane/EtOAc : 80/20); ^{1}H NMR (300 MHz, $CDCl_3$) : δ = 7.34 (m, 15H); 5.93 (m, 1H); 5.32 (dd, *J* = 17.2, 1.5 Hz, 1H); 5.22 (d, *J* = 10.0 Hz, 1H); 4.86 (d, *J* = 4.9 Hz, 0.75H, $H_{1\beta}$); 4.45 (d, *J* = 7.8 Hz, 0.25H, $H_{1\alpha}$); 5.10-4.54 (m, 6H), 4.25-3.47 (m, 10H); 2.52 (t, *J* = 6.3 Hz, 2H); 1.45 (s, 9H); ^{13}C NMR (75 MHz, $CDCl_3$) : δ = 170.7, 138.9, 138.4, 138.2, 133.8, 128.5, 128.4, 128.3, 128.1, 128.0, 127.9, 127.7, 127.5, 118.2, 95.7, 82.1, 80.5, 79.9, 77.6, 75.7, 75.0, 73.2, 70.2, 69.5, 68.2, 67.1, 36.1, 28.1; Anal. Calcd for $C_{37}H_{46}O_8$: C, 71.82; H, 7.49; Found C, 71.75; H, 7.65; MS (ESI, ion polarity positive, MeOH) : m/z: 641.4 $[M+Na]^+$.

tert-Butyl 3-[(3,4,5-tribenzyloxy-6-hydroxy-tetrahydropyran-2-yl)methoxy]propanoate (6). To a stirred mixture of **5** (7.10 g, 11.47 mmol) in CH_3OH /EtOH 2/1 (60 mL) was added $PdCl_2$ (170 mg, mass 2.4%) at room temperature. The brown suspension was stirred under azote atmosphere overnight and became darker and finally black. The reaction mixture was filtered through a pad of Celite which was washed several times with CH_3OH. The filtrate was then concentrated under reduced pressure to obtain a brown oil, which was purified by column chromatography on silica gel with eluent cyclohexane/EtOAc 90/10 to yield **6** as a yellow oil (4.61 g, 75%, α/β 70/30). R_f = 0.15 (cyclohexane/EtOAc : 90/10) ; ^{1}H NMR (300 MHz, $CDCl_3$) : δ = 7.32 (m, 15H); 5.32 (s, 0.70H, $H_{1\beta}$); 5.04- 4.56 (m, 6.30H, 6H+$H_{1\alpha}$); 4.22-3.36 (m, 8H); 2.52 (t, *J* = 6.5 Hz, 2H); 1.45 (s, 9H) ; ^{13}C NMR (75 MHz, $CDCl_3$) : δ = 170.7, 138.9, 138.4, 138.2,

1
2
3
4
5
6
7
8
9
10
11
12
13
14
15
16
17
18
19
20
21
22
23
24
25
26
27
28
29
30
31
32
33
34
35
36
37
38
39
40
41
42
43
44
45
46
47
48
49
50
51
52
53
54
55
56
57
58
59
60

128.5, 128.4, 128.3, 128.1, 128.0, 127.9, 127.7, 127.5, 95.7, 82.1, 80.5, 79.9, 77.6, 75.7, 75.0, 73.2, 70.2, 69.5, 67.1, 36.1, 28.1; MS (ESI, ion polarity positive, MeOH) : m/z: 601.4 $[M+Na]^+$.

tert-Butyl 3-[[3,4,5-tribenzyloxy-6-(2,2,2-trichloroethan imidoyl)oxy-tetrahydropyran-2-yl]methoxy] propanoate (7). To a solution of **6** (4.61 g, 7.96 mmol) in dry CH_2Cl_2 (80 mL) cooled at 0°C was gradually added under azote atmosphere NaH (60% dispersion in mineral oil, 180 mg; 4.50 mmol). Then trichloroacetonitrile (3.8 mL, 38.06 mmol, 11 eq.) was added. After 20 minutes, the ice bath was removed and the reaction mixture was let to stir at room temperature for 4 hours. The solution turned from yellowish to orange while stirring and finally became brown. After stirring overnight, the solvent was evaporated under reduced pressure and the crude residue was purified by column chromatography on neutral alumina with eluent cyclohexane/EtOAc 80/20 to give **7** as a yellow oil (4.31 g, 75%, α/β 85/15). R_f = 0.45 (cyclohexane/EtOAc : 80/20) ; ^1H NMR (300 MHz, $CDCl_3$) : δ = 8.59 (s, 1H); 7.31 (m, 15H); 6.53 (d, J = 3.4 Hz, 0.84H, $H_{1\beta}$); 5,03-4.61 (m, 6.16H, 6H+$H_{1\alpha}$); 4,27-3.48 (m, 8H); 2.51 (t, J = 6.6 Hz, 2H); 1,44 (s, 9H).

tert-Butyl 3-((6-(3-azidopropoxy)-3,4,5-tris(benzyloxy)-tetrahydropyran-2-yl)methoxy) propanoate (8). To a stirred solution of **7** (4.31 g, 5.96 mmol) and 3-azidopropan-1-ol (723 mg, 7.15 mmol) in dry CH_2Cl_2 (15 mL) under azote atmosphere, was added AuCl (181 mg, mass 10%). The reaction mixture was stirred for 2 days at room temperature under azote atmosphere. Upon completion of the reaction monitored by TLC, the mixture was filtered to remove the catalyst and the filtrate was concentrated under reduced pressure. The oily residue afforded was purified by column chromatography on silica gel with eluent cyclohexane/EtOAc 80/20 to give **8** as a yellow oil (3.25 g, 82%, α/β 50/50). R_f = 0.45 (cyclohexane/EtOAc : 80/20) ; ^1H NMR (300 MHz, $CDCl_3$) : δ = 7.33 (m, 15H); 5.08-4.55 (m, 6.50H, 6H+$H_{1\beta}$); 4.38 (d, J = 7.8 Hz, 0.50H,

1
2
3
4
5
6
7
8
9
10
11
12
13
14
15
16
17
18
19
20
21
22
23
24
25
26
27
28
29
30
31
32
33
34
35
36
37
38
39
40
41
42
43
44
45
46
47
48
49
50
51
52
53
54
55
56
57
58
59
60

$H_{1\alpha}$); 4.13-3.23 (m, 12H); 2.51 (t, J = 6.6 Hz, 2H); 1.91 (m, 2H); 1.45 (s, 9H) ; ^{13}C NMR (75 MHz, $CDCl_3$) : δ = 170.8, 138.9, 138.6, 138.4, 138.2, 128.4, 128.3, 128.0, 127.8, 127.6, 103.6 ($C_{1H\alpha}$), 97.2 ($C_{1H\beta}$), 84.7, 82.3, 82.0, 80.5, 80.1, 77.8, 76.6, 75.6, 75.1, 74.9, 73.3, 70.4, 69.8, 69.5, 67.3, 66.6, 64.7, 48.4, 36.3, 36.1, 29.3, 28.9, 28.1, 27.0 ; IR (neat) : 2096 (N_3); 1728 (C=O); 1366 (CH_3); 1066 (C-O) cm^{-1} ; Anal. Calcd for $C_{37}H_{47}N_3O_8 \cdot 0.5\ H_2O$: C, 66.25; H, 7.23; N, 6.27 Found C, 66.11; H, 7.04; N, 5.81 ; MS (ESI, ion polarity positive, MeOH) : m/z: 684.7 $[M+Na]^+$.

3-((6-(3-Azidopropoxy)-3,4,5-tris(benzyloxy)-tetrahydropyran-2-yl)methoxy)propanoic acid (9). To a stirred solution of **8** (3.21 g, 4.85 mmol) in dry CH_2Cl_2 (40 mL) cooled at 0°C was cautiously added TFA (18.6 mL, 250.40 mmol). The reaction mixture appeared like a yellow solution and was stirred overnight at room temperature. The day after, the solvent was evaporated under reduced pressure and the crude residue was purified by column chromatography on silica gel beginning with CH_2Cl_2 100% as eluent and finishing with an eluent mixture CH_2Cl_2/CH_3OH 95/5 to provide **9** as a yellow oil (2.11 g, 72%, α/β 50/50). R_f = 0.40 (CH_2Cl_2/CH_3OH 95/5) ; ^{1}H NMR (300 MHz, $CDCl_3$) : δ = 7.32 (m, 15H); 6.93 (s, 1H); 5.04-4.54 (m, 6.50H, 6H+$H_{1\beta}$); 4.40 (d, J = 7.8 Hz, 0.50H, $H_{1\alpha}$); 4.08-3.32 (m, 12H); 2.63 (m, 2H); 2.03-1.71 (m, 2H) ; ^{13}C NMR (75 MHz, $CDCl_3$) : δ = 175.4, 138.8, 138.5, 138.4, 138.2, 138.1, 128.4, 128.0, 127.9, 127.6, 103.6 ($C_{1H\alpha}$), 97.2 ($C_{1H\beta}$), 84.6, 82.2, 82.0, 80.1, 75.7, 75.1, 74.9, 74.6, 73.3, 70.2, 69.9, 69.7, 66.6, 64.8, 48.3, 34.7, 34.5, 29.3, 28.9; IR (neat) : 2097 (N_3); 1714 (C=O); 1065 (C-O) cm^{-1}; MS (ESI, ion polarity positive, MeOH) : m/z: 629 $[M+Na]^+$.

N-[(1*S*)-1-[[(5-Acetamido-2-methoxy-benzoyl)amino]carbamoyl]-2-methyl-propyl]-3-[[(3*S*,4*S*,5*S*)-3,4,5-tribenzyloxy-6-[3-[(imino-5-azanylidene)amino]propoxy] tetrahydropyran-2-yl]methoxy]propanamide (12). To a stirred solution of **10** (360 mg, 0.83

1
2
3
4
5
6
7
8
9
10
11
12
13
14
15
16
17
18
19
20
21
22
23
24
25
26
27
28
29
30
31
32
33
34
35
36
37
38
39
40
41
42
43
44
45
46
47
48
49
50
51
52
53
54
55
56
57
58
59
60

mmol) in dry DMF (5 mL) and cooled at 0°C under azote atmosphere, were successively added DMTMM (270 mg, 0.83 mmol) and NMM (272 µL, 2.48 mmol). The reaction mixture was stirred at 0°C for 1h. Then, 9 (500 mg, 0.83 mmol) in dry DMF (5 mL) was added to the reaction mixture. The ice bath was removed after 30 minutes and the orange reaction mixture was stirred at room temperature overnight. The solvent was evaporated under reduced pressure and the oily residue was taken up with EtOAc (50 mL). The organic layer was successively washed with distilled water, 10% citric acid aqueous solution, 10% aqueous K_2CO_3 solution and brine, dried over anhydrous Na_2SO_4, filtered and concentrated under reduced pressure. The yellow crude product was purified by puriflash column chromatography (SI-HP, 12 g, 22 bars, 30 µm, flow rate: 20 mL/min) with eluent CH_2Cl_2/CH_3OH 95/5 to afford **12** as a white solid (593 mg, 86%, α/β 40/60); mp = 71-73 °C ; R_f = 0.60 (CH_2Cl_2/CH_3OH 95/5) ; ^1H NMR (300 MHz, $CDCl_3$) : δ = 12.05 (t, J = 6.2 Hz, 1H, NH); 11.28 (d, J = 6.3 Hz, 1H, NH); 9.80 (s, 1H); 8.58 (dd, J = 9.1, 2.4 Hz, 1H); 8.27 (d, J = 2.4 Hz, 1H); 7.33-7.19 (m, 15H); 7.07-6.95 (m,2H); 5.30 (m, 1H); 4.94-4.58 (m, 6.40H, 6H+$H_{1\beta}$); 4.40 (d, J = 7.8 Hz, 0.60H, $H_{1\alpha}$); 4.02-3.44 (m, 15H); 2.59 (m, 2H); 2.19 (s, 3H); 2.09-2.01 (m, 1H); 1.94-1.83 (m, 2H); 0.91-0.96 (m, 6H) ; ^{13}C NMR (75 MHz, $CDCl_3$) : δ = 171.2, 171.1, 169.0, 164.9, 158.2, 158.1, 153.1, 138.9, 138.6, 138.4, 138.3, 138.2, 138.1, 133.9, 128.4, 128.3, 128.0, 127.9, 127.8, 127.5, 124.7, 122.5, 117.7, 111.8, 103.6 ($C_{1H\alpha}$), 97.1 ($C_{1H\beta}$), 84.6, 82.3, 81.9, 80.3, 77.8, 77.7, 75.5, 75.1, 75.0, 74.9, 73.1, 70.3, 70.1, 69.7, 67.7, 67.6, 66.6, 64.8, 56.4, 55.8, 48.3, 37.6, 37.5, 33.4, 33.3, 29.3, 28.9, 24.3, 18.9, 18.2 ; IR (neat) : 3375 (N-H); 2097 (N_3) cm^{-1}; Anal. Calcd for $C_{48}H_{59}N_7O_{11} \cdot 0.5\ H_2O$: C, 62.73; H, 6.58; N, 10.67 Found C, 62.78; H, 6.98; N, 10.55 ; MS (ESI, ion polarity negative, MeOH) : m/z: 908.0 $[M{-}H]^-$.

Benzyl *N*-[(5*S*)-6-[2-(5-acetamido-2-methoxy-benzoyl)hydrazino]-6-oxo-5-[3-[[(3*S*,4*S*,5*S*)-3,4,5-tribenzyloxy-6-[3-[(imino-5-azanylidene)amino]propoxy]tetrahydropyran-2-yl]methoxy] propanoylamino]hexyl]carbamate (13). Same procedure as described for **12** from **11b** (495 mg, 0.826 mmol) and 9 (500 mg, 0.826 mmol). The yellow crude product obtained was purified by puriflash column chromatography (SI-HP, 12 g, 22bar, 30 µm, flow rate: 20 mL/min) with eluent CH_2Cl_2/CH_3OH 95/5 to afford **13** as a white solid (593 mg, 68%, α/β 50/50). R_f = 0.15 et 0.25 (two diastereoisomers) (CH_2Cl_2/CH_3OH 95/5) ; ^{1}H NMR (300 MHz, $CDCl_3$) : δ = 11.97 (sl, 1H, NH) ; 11.32 (sl, 1H, NH); 9.80 (sl, 1H, NH); 8.58 (d, *J* = 7.7 Hz, 1H); 8.17 (s, 1H); 7.32 - 7.26 (m, 21H); 6.91 (m, 1H); 5.41 (m, 1H); 5.07 – 4.60 (m, 9.50H, 9H+$H_{1\beta}$); 4.42 (d, *J* = 7.8 Hz, 0.50H, $H_{1\alpha}$); 4.11 – 3.32 (m, 15H); 2.99 (m, 2H); 2.59 (s, 2H); 2.21 (s, 3H); 1.88 (m, 2H); 1.37 (m, 6H) ; ^{13}C NMR (75 MHz, $CDCl_3$) : δ = 174.2, 173.3, 169.2, 165.5, 156.3, 153.3, 138.5, 138.0, 137.8, 136.7, 133.8, 128.5, 128.3, 128.0, 127.8, 125.0, 122.1 (C_{30}), 117.7, 111.9, 103.6 ($C_{1H\alpha}$), 97.2 ($C_{1H\beta}$), 92.2, 87.2, 84.6, 82.0, 81.7, 75.6, 66.7 (C_{16}), 56.4, 50.8, 48.3, 40.6, 37.6, 34.1, 34.0, 33.9, 29.1, 24.0, 22.2, 20.48; MS (ESI, ion polarity positive, MeOH) : m/z: 1095.48 $[M+Na]^+$.

***N*-[(1*S*)-1-[[(5-Acetamido-2-methoxy-benzoyl)amino]carbamoyl]-2-methyl-propyl]-3-[[(3*S*,4*S*,5*S*)-6-(3-aminopropoxy)-3,4,5-tribenzyloxy-tetrahydropyran-2-yl]methoxy]propanamide (14).** To a stirred solution of **12** (174 mg, 0.19 mmol) in THF (2 mL) was added at room temperature Ph_3P (100 mg, 0.38 mmol). After 10 minutes, H_2O (0.3 mL) was added and the reaction was stirred at reflux at 40°C for 24 h. The solvents were evaporated under reduced pressure and the oily residue obtained was purified by column chromatography on silica gel successively eluting with CH_2Cl_2 100%, then CH_2Cl_2/CH_3OH 95/5, CH_2Cl_2/CH_3OH 90/10 to eliminate the impurities and finally with $CH_2Cl_2/CH_3OH/NH_4OH$ (20% aq. sol.) 88/9/3 to

afford **14** (107 mg, 63%, α/β 40/60) as a white solid; mp = 203-205 °C ; R_f = 0.10 ($CH_2Cl_2/CH_3OH/NH_4OH$ (20% aq. sol.) 88/9/3 ; ^{1}H NMR (300 MHz, $CDCl_3$) : δ = 9.71 (bs, 1H); 8.55 (dd, *J* = 9.1, 2.7 Hz, 1H); 8.25 (d, *J* = 2.7 Hz, 1H); 7.31-7.20 (m, 16H); 6.92 (d, *J* = 9.1, 1H); 5.25 (m, 1H); 4.89-4.57 (m, 6,40 H, 6H+$H_{1\beta}$); 4.41 (d, *J* = 7.8 Hz, 0.60H, $H_{1\alpha}$); 3.94 (s, 3H); 3.91 – 3.36 (m, 12H); 2.85 (m, 2H); 2.58 (m, 2H); 2.17 (s, 3H); 2.08 (m, 1H); 1.78 (m, 2H); 0.91 (m, 6H) ; ^{13}C NMR (75 MHz, $CDCl_3$) : δ = 171.3, 169.0, 165.4, 158.4, 153.1, 138.6, 138.5, 138.0, 133.9, 128.4, 128.3, 128.0, 127.8, 127.6, 127.5, 124.8, 122.5, 117.8, 111.8, 103.6, 84.6, 82.3, 77.9, 75.5, 75.0, 74.8, 70.2, 67.7, 56.4, 56.0, 38.9, 37.5, 33.2, 33.0, 24.3, 19.0, 18.3 ; IR (neat) : 3465, 3418 (HN-H) cm^{-1}; Anal. Calcd for $C_{48}H_{61}N_5O_{11} \cdot (CH_3)_2CO$: C, 65.02; H, 7.18; N, 7.44 Found C, 64.88; H, 7.55; N, 7.16 ; MS (ESI, ion polarity negative, MeOH) : m/z: 882.7 $[M–H]^-$.

Benzyl *N*-[(5*S*)-6-[2-(5-acetamido-2-methoxy-benzoyl)hydrazino]-5-[3-[[(3*S*,4*S*,5*S*)-6-(3-aminopropoxy)-3,4,5-tribenzyloxy-tetrahydropyran-2-yl]methoxy]propanoylamino]-6-oxo-hexyl]carbamate (15). Same procedure as described for **14** from **13** (497 mg, 0.463 mmol) to afford 15 (247 mg, 50%, α/β 50/50) as a white solid. R_f = 0.1 ($CH_2Cl_2/CH_3OH/NH_4OH$ (20% aq. sol.) 88/9/3) ; ^{1}H NMR (300 MHz, CD_3OD) : δ = 8.08 (dd, *J* = 12.4, 2.7 Hz, 1H); 7.70 (m, 1H); 7.34-7.22 (m, 20H); 6.98 (m, 1H); 4.98 (s, 2H); 4.97 – 4.53 (m, 8.50H, 8H+$H_{1\beta}$); 4.41 (m, 1H), 4.37 (d, *J* = 7.7 Hz, 0.50H, $H_{1\alpha}$); 3.86 (s, 3H), 3.80 – 3.21 (m, 10H) 3.04 (m, 2H); 2.85 (m, 2H) 2.48 (m, 2H); 2.03 (m, 3H); 1.87 – 1.67 (m, 4H); 1.42 (m, 4H) ; ^{13}C NMR (75 MHz, CD_3OD) : δ = 173.9, 171.5, 171.3, 164.6, 164.2, 158.8, 155.5, 140.0, 139.9, 139.6, 139.5, 138.3, 133.5, 129.4-128.6, 126.6, 126.3, 124.3, 124.2, 121.3, 121.2, 113.4, 104.7 ($C_{1H\alpha}$), 98.0 ($C_{1H\beta}$), 85.6, 83.4, 83.0, 81.4, 79.1, 78.9, 76.4, 76.0, 75.9, 75.6, 75.3, 74.0, 71.7, 70.7, 68.6, 68.5, 68.3, 67.5, 67.3, 56.9, 53.8, 53.7, 49.9, 41.5, 39.8, 39.3, 37.5, 37.3, 33.0, 32.9, 30.9, 30.4, 24.0, 23.9, 23.7 ;

1
2
3
4
5
6
7
8
9
10
11
12
13
14
15
16
17
18
19
20
21
22
23
24
25
26
27
28
29
30
31
32
33
34
35
36
37
38
39
40
41
42
43
44
45
46
47
48
49
50
51
52
53
54
55
56
57
58
59
60

HRMS (TOF, ESI, ion polarity positive, H_2O/ MeOH): m/z $[M+H]^+$, calcd for $C_{57}H_{71}N_6O_{13}$ 1047.5079; found 1047.5063.

tert-Butyl *N*-[(1*S*)-1-[3-[6-[[3-[[(1S)-1-[[(5-acetamido-2-methoxy-benzoyl)amino] carbamoyl]-2-methyl-propyl]amino]-3-oxo-propoxy]methyl]-3,4,5-tribenzyloxy-tetrahydropyran-2-yl]oxypropylcarbamoyl]-2-methyl-propyl]carbamate (16). To a stirred solution of *N*-Boc-Val-OH (132 mg, 0.60 mmol) in dry DMF (2 mL) and cooled at 0 °C, under azote atmosphere, were successively added DMTMM (98.4 mg, 0.30 mmol) and NMM (100 µL, 0.91 mmol). The reaction mixture was stirred at 0 °C for 1h. Then **14** (270 mg, 0.30 mmol) in dry DMF (2 mL) was added to the reaction mixture. The ice bath was removed after 30 minutes and the orange reaction mixture was stirred at room temperature overnight. The solvent was evaporated under reduced pressure and the oily residue obtained was taken up with EtOAc (50 mL). The organic layer was successively washed with distilled water, 10% citric acid aqueous solution, 10% K_2CO_3 aqueous solution, and brine, dried over anhydrous Na_2SO_4, filtered and concentrated under reduced pressure. The oily crude product was purified by puriflash column chromatography (SI-HP, 12 g, 22 bars, 30 µm, flow rate: 20 mL/min) with eluent CH_2Cl_2/CH_3OH 95/5 to afford **16** (260 mg, 79%, α/β 40/60) as a white solid. R_f = 0.35 (CH_2Cl_2/CH_3OH 95/5) ; ^1H NMR (300 MHz, CD_3OD) : δ = 8.04 (s, 1H); 7.80 (d, *J* = 8.8, 2.7 Hz, 1H); 7.34-7.25 (m, 15H); 7.10 (d, *J* = 8.8 Hz, 1H); 4.93-4.61 (m, 6.40H, 6H+$H_{1\beta}$); 4.44 (d, *J* = 7.8 Hz, 0.60H, $H_{1\alpha}$); 4.34 (d, *J* = 6.8 Hz, 1H); 3.94 (s, 3H); 3.81-3.29 (m, 13H); 2.61-2.46 (m, 2H); 2.14-2.09 (m, 4H); 199-1.79 (m, 3H); 1.45 (s, 9H); 1.04 (dd, *J* = 11.2, 6.7 Hz, 6H); 0.93 (m, 6H) ; ^{13}C NMR (75 MHz, CD_3OD) : δ = 174.4, 174.2, 171.5, 171.4, 157.9, 155.6, 140.3, 139.9, 139.6, 133.5, 129.5, 129.3, 129.0, 128.9, 128.6, 128.5, 126.7, 124.3, 121.2, 113.4, 104.8 ($C_{1H\alpha}$), 98.1 ($C_{1H\beta}$), 83.0, 81.4, 78.9, 76.4, 76.0, 75.9, 75.8, 73.9, 71.6, 70.5, 68.6, 67.4, 61.8, 58.9, 57.0,

1 2 3 4 5 6 7 8 9 10 11 12 13 14 15 16 17 18 19 20 21 22 23 24 25 26 27 28 29 30 31 32 33 34 35 36 37 38 39 40 41 42 43 44 45 46 47 48 49 50 51 52 53 54 55 56 57 58 59 60

38.0, 37.5, 32.0, 31.6, 30.3, 28.7, 23.6, 19.8, 18.9, 18.6; MS (ESI, ion polarity negative, MeOH) : m/z: 1081.9 $[M–H]^-$.

tert-Butyl *N*-[(1*S*)-2-[[(1*S*)-1-[3-[(3*S*,4*S*,5*R*)-6-[[3-[[(1*S*)-1-[[(5-acetamido-2-methoxy-benzoyl)amino]carbamoyl]-5-(benzyloxycarbonylamino)pentyl]amino]-3-oxo-propoxy]methyl]-3,4,5-tribenzyloxy-tetrahydropyran-2-yl]oxypropylcarbamoyl]-2-methyl-propyl]amino]-1-methyl-2-oxo-ethyl]carbamate (17). Same procedure as described for **16** from **15** (245 mg, 0.234 mmol) to afford **17** as a white solid (200 mg, 68%, α/β 50/50). R_f = 0.35 et 0.40 (two diastereoisomers) (CH_2Cl_2/CH_3OH : 95/5) ; ^1H NMR (300 MHz, CD_3OD) : δ = 8.06 (s, 1H) ; 7.83 (m, 1H); 7.29-7.23 (m, 20H); 7.04 (dd, *J* = 9.0, 3.6 Hz, 1H); 5.03 (m, 2H); 4.91 – 4.57 (m, 6.50H, 6H+$H_{1β}$); 4.51 (m, 1H); 4.40 (d, *J* = 7.8 Hz, 0.50H, $H_{1α}$); 3.88 (s, 3H); 3.84 – 3.48 (m, 10H); 3.43-3.28 (m, 3H); 3.08 (m, 2H); 2.53 (m, 2H); 2.08 (m, 3H); 2.00 – 1.78 (m, 5H); 1.49 (m, 4H); 1.42 (s, 9H); 0.90 (m, 6H) ; ^{13}C NMR (75 MHz, CD_3OD) : δ = 174.3, 174.1, 174.0, 172.1, 171.4, 165.3, 158.8, 157.8, 155.5, 140-139.6, 138.4, 133.6, 129.4- 128.5, 126.8, 124.3, 120.9, 113.4, 104.8 ($C_{1Hα}$), 98.1 ($C_{1Hβ}$), 85.7, 83.5, 83.0, 81.6, 80.5, 79.1, 76.5, 76.0, 75.7, 73.9, 71.6, 70.8, 70.6, 68.5, 67.3, 61.7, 61.6, 57.0, 53.3, 41.5, 37.6, 32.8, 32.7, 32.1, 30.7, 30.4, 28.7, 24.0, 23.9, 23.7, 19.8, 18.6 ; MS (ESI, ion polarity positive, MeOH) : m/z: 1268.61 $[M+Na]^+$. HRMS (TOF, ESI, ion polarity positive, H_2O/ MeOH): m/z $[M+Na]^+$, calcd for $C_{67}H_{87}N_7O_{16}Na$ 1268.6102; found 1268.6093.

tert-Butyl *N*-[(1S)-2-[[(1S)-1-[3-[6-[[3-[[(1S)-1-[[(5-acetamido-2-methoxy-benzoyl)amino]carbamoyl]-2-methyl-propyl]amino]-3-oxo-propoxy]methyl]-3,4,5-tribenzyloxy-tetrahydropyran-2-yl]oxypropylcarbamoyl]-2-methyl-propyl]amino]-1-methyl-2-oxo-ethyl]carbamate (18). To a stirred solution of **16** (270 mg, 0.25 mmol) in dry CH_2Cl_2 (2 mL), cooled to 0 °C was carefully added TFA (1 mL). After 30 minutes the ice bath

1
2
3
4
5
6
7
8
9
10
11
12
13
14
15
16
17
18
19
20
21
22
23
24
25
26
27
28
29
30
31
32
33
34
35
36
37
38
39
40
41
42
43
44
45
46
47
48
49
50
51
52
53
54
55
56
57
58
59
60

was removed and the reaction mixture was stirred at room temperature for 3 h. The solvent was evaporated at reduced pressure and the viscous oily residue was taken up with toluene and again evaporated. The oily residue obtained was triturated in Et_2O to yield the TFA salt of the free amine **16a** (301 mg, quantitative, α/β 50/50) as a white solid. R_f = 0 (CH_2Cl_2/CH_3OH : 95/5) ; ^{1}H NMR (300 MHz, CD_3OD) : δ = 8.06 (m, 1H); 7.72 (dd, *J* = 8.7, 2.8 Hz, 1H); 7.28-7.21 (m, 15H); 7.03 (dd, *J* = 9.0, 2.3 Hz, 1H); 4.86-4.56 (m, 6.50H, 6H+$H_{1β}$); 4.44 (d, *J* = 7.8 Hz, 0.50H, $H_{1α}$); 4.37 (d, *J* = 6.9, 1H); 3.91 (s, 3H); 3.80-3.34 (m, 13H); 2.50 (m, 2H); 2.12 (m, 2H); 2.06 (s, 3H); 1.80 (m, 2H); 1.02-0.95 (m, 12H) ; ^{13}C NMR (75 MHz, CD_3OD) : δ = 174.2, 171.4, 171.4, 169.3, 165.4, 155.5, 140.1, 140.0, 139.9, 139.7, 139.5, 133.5, 129.4, 129.3, 129.2, 129.0, 128.9, 128.7, 128.5, 126.8, 124.3, 121.0, 113.4, 104.8 ($C_{1Hα}$), 98.1 ($C_{1Hβ}$), 85.7, 83.0, 81.4, 80.6, 78.9, 76.3, 76.1, 75.7, 75.5, 71.6, 73.9, 71.6, 70.6, 68.2, 67.0, 59.9, 58.8, 56.9, 38.0, 37.8, 37.4, 32.0, 31.9, 31.4, 30.3, 23.6, 19.7, 18.9, 18.8, 18.1, 17.9 ; MS (ESI, ion polarity negative, MeOH) : m/z: 983.53 $[M+H]^+$.

Same procedure as described for **12** from *N*-Boc-L-Ala-OH (102.6 mg, 0.55 mmol, 2 eq.) and **16a** (300 mg, 0.273 mmol) to afford **18** as a white solid (210 mg, 68%, α/β 50/50). R_f = 0.20 (CH_2Cl_2/CH_3OH : 95/5) ; ^{1}H NMR (300 MHz, CD_3OD) : δ = 8.04 (d, *J* = 2.8 Hz, 1H); 7.85 (m, 1H); 7.40-7.19 (m, 15H); 7.11 (m, 1H); 5.00-4.69 (m, 6.50 H, 6H+$H_{1β}$); 4.43 (d, *J* = 7.9 Hz, 0.50H, $H_{1α}$); 4.38 (d, *J* = 6.9 Hz, 1H); 4.22-4.06 (m, 2H); 3.95 (s, 3H); 3.84-3.28 (m, 12H); 2.67-2.44 (m, 2H); 2.25-2.11 (m, 5H); 1.83 (m, 2H); 1.44 (s, 9H); 1.30 (m, 3H); 1.05 (m, 6H); 0.93 (m, *J* = 6.5 Hz, 6H) ; ^{13}C NMR (75 MHz, $CDCl_3$) : δ = 172.8, 172.7, 171.1, 171.0, 169.0, 165.3, 158.5, 153.1, 138.8, 138.5, 138.4, 138.1,133.7, 128.4, 128.3, 128.2, 127.9, 127.8, 127.7, 127.4, 124.9, 122.5, 117.8, 111.8, 103.6 ($C_{1Hα}$), 97.1 ($C_{1Hβ}$), 84.5, 82.1, 82.0, 80.1, 80.0, 77.7, 75.5, 75.4, 74.9, 74.7, 74.6, 73.2, 70.2, 70.0, 69.9, 67.9, 67.6, 67.4, 66.7, 58.5, 56.4, 55.9, 50.3, 37.4,

37.3, 33.0, 31.0, 30.9, 29.2, 28.2, 24.2, 19.3, 18.9, 18.2, 17.7 ; HRMS (TOF, ESI, ion polarity positive, H_2O/ MeOH): m/z $[M+Na]^+$, calcd for $C_{61}H_{83}N_7O_{15}Na$ 1176.5839; found 1176.5827.

tert-Butyl *N*-[(1*S*)-2-[[(1*S*)-1-[3-[(3*S*,4*S*,5*R*)-6-[[3-[[(1S)-1-[[(5-acetamido-2-methoxy-benzoyl)amino]carbamoyl]-5-(benzyloxycarbonylamino)pentyl]amino]-3-oxo-propoxy]methyl]-3,4,5-tribenzyloxy-tetrahydropyran-2-yl]oxypropylcarbamoyl]-2-methyl-propyl]amino]-1-methyl-2-oxo-ethyl]carbamate (19).

Same procedure as described for **18** from **17** (200 mg, 0.16 mmol) to afford the TFA salt of the free amine **17a** as a white solid (207 mg, quantitative, α/β 50/50). R_f = 0 (CH_2Cl_2/CH_3OH : 95/5) ; ^1H NMR (300 MHz, CD_3OD) : δ = 8.14 (m, 1H) ; 7.74 (d, *J* = 9.0 Hz, 1H); 7.35 – 7.23 (m, 20H); 7.12 (d, *J* = 9.0 Hz, 1H); 5.03 (s, 2H); 4.88 – 4.48 (m, 7.50H, 7H+$H_{1\beta}$); 4.41 (d, *J* = 7.9 Hz, 0.50H, $H_{1\alpha}$); 3.90 (s, 3H); 3.89 – 3.20 (m, 13H); 3.07 (m, 2H); 2.55 (m, 2H); 2.13 (m, 1H), 2.08 (m, 3H); 1.93– 1.75 (m, 4H); 1.51 (m, 4H); 1.02 (m, 6H) ; ^{13}C NMR (75 MHz, CD_3OD) : δ = 174.2, 172.2, 171.5, 169.4, 165.5, 158.8, 155.6, 140.1, 139.9, 139.7, 138.4, 133.5, 129.4-128.6, 126.8, 124.3, 120.9, 113.5, 104.8 ($C_{1H\alpha}$), 98.0 ($C_{1H\beta}$), 85.7, 83.4, 83.0, 81.6, 79.0, 76.5, 76.1, 75.9, 75.6, 73.9, 71.6, 70.7, 68.5, 68.3, 67.3, 67.0, 59.9, 57.0, 53.4, 41.5, 37.8, 37.5, 32.7, 31.4, 30.4, 24.0, 23.7, 18.9, 18.1, 18.0; HRMS (TOF, ESI, ion polarity positive, H_2O/ MeOH): m/z $[M+H]^+$, calcd for $C_{62}H_{80}N_7O_{14}$ 1146.5763; found 1146.5752.

Same procedure as described for **12** from *N*-Boc-L-Ala-OH (59.5 mg, 0.32 mmol) and **17a** (200 mg, 0.16 mmol) to afford **19** as a white solid (152 mg, 73%, α/β 50/50). R_f = 0.30 (CH_2Cl_2/CH_3OH : 95/5) ; ^1H NMR (300 MHz, CD_3OD) : δ = 8.05 (m, 1H) ; 7.82 (s, 1H) ; 7.38 – 7.23 (m, 20H); 7.11 (m, 2H); 5.05 (m, 2H); 4.91 – 4.59 (m, 6.50H, 6H+$H_{1\beta}$); 4.49 (m, 1H); 4.40 (d, *J* = 7.8 Hz, 0.50H, $H_{1\alpha}$); 4.10 (m, 2H); 3.92 (s, 3H); 3.89 (m, 1H); 3.76 – 3.31 (m, 11H); 3.09 (s, 2H); 2.54 (s, 2H); 2.09 (m, 3H); 2.02 (m, 1H); 1.91 – 1.78 (m, 4H,); 1.49 (m, 4H); 1.41 (s,

1 2 3 4 5 6 7 8 9 10 11 12 13 14 15 16 17 18 19 20 21 22 23 24 25 26 27 28 29 30 31 32 33 34 35 36 37 38 39 40 41 42 43 44 45 46 47 48 49 50 51 52 53 54 55 56 57 58 59 60

9H); 1.28 (s, 3H); 0.91 (m, 6H) ; ^{13}C NMR (75 MHz, CD_3OD) : δ = 175.8, 174.2, 172.2, 172.0, 171.5, 169.4, 165.5, 164.3, 158.7, 155.7, 140.1, 138.6, 133.5, 129.4,129.3, 129.2, 129.0, 128.9, 128.5, 126.9, 124.3, 120.9, 113.5, 104.8 ($C_{1H\alpha}$), 98.0 ($C_{1H\beta}$), 83.4, 81.6, 80.8, 79.1, 76.5, 76.1, 75.9, 73.9, 71.6, 70.7, 68.5, 67.3, 67.2, 60.0, 57.0, 53.4, 51.7, 44.6, 41.5, 37.9, 37.5, 32.6, 32.1, 30.6, 30.4, 28.7, 23.9, 23.7, 19.1, 18.4, 18.0, 17.9 ; MS (ESI, ion polarity positive, MeOH) : m/z: 1339,65 $[M+Na]^+$. HRMS (TOF, ESI, ion polarity positive, H_2O/ MeOH): m/z $[M+H]^+$, calcd for $C_{70}H_{92}N_8O_{17}Na$ 1339.6478; found 1339.6483. HPLC purity: TR (α,β) = 23.54, 23.87 min., 93.5 %.

tert-Butyl N-[(1*S*)-2-[[(1*S*)-1-[3-[(3*S*,4*S*,5*S*)-6-[[3-[[(1*S*)-1-[[(5-acetamido-2-methoxy-benzoyl)amino]carbamoyl]-2-methyl-propyl]amino]-3-oxo-propoxy]methyl]-3,4,5-trihydroxy-tetrahydropyran-2-yl]oxypropylcarbamoyl]-2-methyl-propyl]amino]-1-methyl-2-oxo-ethyl]carbamate (20). To a stirred solution of **18** (105 mg, 0.091 mmol) in CH_3OH (3 mL) was added Pd/C (25 mg, 25% mass). The reaction flask was purged three times with hydrogen, and stirring was maintained under hydrogen atmosphere at room temperature for 2 days. Upon completion of the reaction monitored by TLC, the solution was filtered through a pad of Celite which was washed several times with CH_3OH. Then, the filtrate was concentrated under reduced pressure to provide **20** (70.7 mg, 88%, α/β 50/50) as a white solid. R_f = 0 (CH_2Cl_2/ CH_3OH : 95/5); ^{1}H NMR (300 MHz, CD_3OD) : δ = 7.97 (s, 1H); 7.77 (dd, *J* = 9.0, 2.2 Hz, 1H); 7.07 (d, *J* = 9.0 Hz, 1H); 4.71 (d, *J* = 3.6 Hz, 0.50H, $H_{1\beta}$); 4.35 (d, *J* = 6.9 Hz, 1H); 4.21 (d, *J* = 7.8 Hz, 0.50H, $H_{1\alpha}$); 4.08 (m, 1H); 3.93 (s, 3H); 3.75-3.24 (m, 12H); 2.52 (m, 2H); 2.13 (m, 1H); 2.08 (s, 3H); 2.00 (m, 1H); 1.75 (m, H); 1.39 (s, 9H); 1.26 (d, *J* = 7.2 Hz, 3H); 1.01 (m, 6H); 0.89 (d, *J* = 6.7 Hz, 6H) ; ^{13}C NMR (75 MHz, CD_3OD) : δ = 175.6, 174.2, 173.2, 171.7, 171.6, 165.5, 155.6, 155.6, 133.4, 126.9, 124.3, 121.1, 113.4, 104.3 ($C_{1H\alpha}$), 100.2 ($C_{1H\beta}$), 80.7,

1
2
3
4
5
6
7
8
9
10
11
12
13
14
15
16
17
18
19
20
21
22
23
24
25
26
27
28
29
30
31
32
33
34
35
36
37
38
39
40
41
42
43
44
45
46
47
48
49
50
51
52
53
54
55
56
57
58
59
60

77.9, 76.7, 75.0, 73.4, 72.5, 71.6, 71.5, 71.3, 71.2, 68.7, 68.6, 67.2, 60.1, 58.8, 58.7, 57.0, 51.7, 37.9, 37.4, 32.0, 32,2, 32.0, 30.0, 28.7, 23.6, 19.7, 18.8, 18.7, 17.9 ; HRMS (TOF, ESI, ion polarity positive, H_2O/ MeOH): m/z $[M+Na]^+$, calcd for $C_{40}H_{65}N_7O_{15}Na$ 906.4436; found 906.4421. HPLC purity: TR (α, β) = 17.56 min., 97.1 %.

tert-Butyl N-[(1*S*)-2-[[(1*S*)-1-[3-[(3*S*,4*S*,5*S*)-6-[[3-[[(1*S*)-1-[[(5-acetamido-2-methoxy-benzoyl)amino]carbamoyl]-5-amino-pentyl]amino]-3-oxo-propoxy]methyl]-3,4,5-trihydroxy-tetrahydropyran-2-yl]oxypropylcarbamoyl]-2-methyl-propyl]amino]-1-methyl-2-oxo-ethyl]carbamate (21). Same procedure as described for **20** from **19** (111 mg, 0.083 mmol) in CH_3OH (3 mL) except that CH_3CO_2H was added (1 mL) to provide **21** (61.6 mg, 75%, α/β 50/50) as a white solid. R_f = 0 (CH_2Cl_2/ CH_3OH : 95/5); ^1H NMR (300 MHz, CD_3OD) : δ = 8.12 (s, 1H); 7.73 (s, 1H); 7.13 (d, *J* = 8.6 Hz, 1H); 4.76 (d, *J* = 3.6 Hz, 0.50H, $H_{1\beta}$); 4.54 (m, 1H), 4.26 (d, *J* = 7.6 Hz, 0.50H, $H_{1\alpha}$); 4.13 (m, 2H); 3.97 (s, 3H); 3.89 – 3.57 (m, 6H); 3.34 – 3.26 (m, 5H); 3.17 (m, 1H); 2.97 (m, 2H); 2.55 (m, 2H); 2.12 (s, 3H); 2.04 (m, 1H); 1.96 (s, 8H, 2H + CH_3CO_2H); 1.78 (m, 4H); 1.56 (m, 2H); 1.43 (s, 9H); 1.29 (m, 3H); 0.93 (d, *J* = 6.6 Hz, 6H) ; ^{13}C NMR (75 MHz, CD_3OD) : δ = 177.3, 175.8, 174.4, 173.3, 171.6, 157.8, 155.7, 133.5, 130.5, 126.9, 124.4, 121.0, 113.5, 104.4 ($C_{1H\alpha}$), 100.3 ($C_{1H\beta}$), 8.7, 77.9, 76.7, 75.1, 73.5, 72.6, 71.6, 71.5, 71.1, 68.6, 67.2, 60.1, 57.0, 53.0, 51.7, 45.8, 40.5, 37.9, 37.7, 37.4, 32.5, 32.2, 30.2, 28.7, 28.1, 26.9, 23.7, 22.1, 19.7, 19.3, 18.6, 17.9; HRMS (TOF, ESI, ion polarity positive, H_2O/ MeOH): m/z $[M+H]^+$, calcd for $C_{41}H_{69}N_8O_{15}$ 913.4882; found 913.4883, m/z $[M+Na]^+$, calcd for $C_{41}H_{68}N_8O_{15}Na$ 935.4702, found 935.4708 ; HPLC purity: TR (α, β) = 12.8, 13.1 min., 88.9 %.

(2*S*)-*N*-[3-[(3*S*,4*S*,5*S*)-6-[[3-[[(1S)-1-[[(5-Acetamido-2-methoxy-benzoyl)amino]carbamoyl]-2-methyl-propyl]amino]-3-oxo-propoxy]methyl]-3,4,5-tribenzyloxy-tetrahydropyran-2-yl]oxypropyl]-2-[[(2S)-2-aminopropanoyl]amino]-3-

1
2
3
4
5
6
7
8
9
10
11
12
13
14
15
16
17
18
19
20
21
22
23
24
25
26
27
28
29
30
31
32
33
34
35
36
37
38
39
40
41
42
43
44
45
46
47
48
49
50
51
52
53
54
55
56
57
58
59
60

methyl-butanamide (22). Same procedure as described for **16a** from **18** (38 mg, 0.033 mmol) in dry CH_2Cl_2 (270 μL) to yield **22** as a white solid (40 mg, quantitative, α/β 50/50). R_f = 0 (CH_2Cl_2/ CH_3OH: 95/5); ^1H NMR (300 MHz, CD_3OD) : δ = 8.12 (m, 1H); 7.77 (d, *J* = 8.9 Hz, 1H); 7.35-7.26 (m, 15H); 7.10 (d, *J* = 8.9 Hz, 1H); 5.07-4.61 (m, 6.50H, 6H+$H_{1\beta}$); 4.44 (d, *J* = 7.9 Hz, 0.50H, $H_{1\alpha}$); 4.40 (m, 1H); 4.17 (m, 1H); 4.02 (m, 1H); 3.94 (s, 3H); 3.86-3.35 (m, 12H); 2.56 (m, 2H); 2.34-1.98 (m, 5H); 1.84 (m, 2H); 1.51-1.47 (m, 3H); 1.30 (s, 3H); 0.99 (m, 12H) ; ^{13}C NMR (75 MHz, CD_3OD) : δ = 174.1, 173.0, 171.0, 171.5, 171.0 165.4, 155.6, 140.2, 140.0, 139.9, 139.7, 139.5, 133.5, 129.4-128.5, 126.8, 124.3 , 121.0, 113.4, 104.8 ($C_{1H\alpha}$), 98.0 ($C_{1H\beta}$), 85.7, 83.2, 83.0, 81.4, 79.0, 76.4, 76.0, 75.9, 75.6, 73.9, 71.7 70.6, 68.5, 68.3, 68.2, 67.3, 60.7, 58.8, 56.9, 50.3, 49.9, 38.0, 37.6, 37.5, 32.0, 31,9, 30.4, 30.4, 23.6, 19.8, 19.0, 18.9, 18.7, 17.8 ; HRMS (TOF, ESI, ion polarity positive, H_2O/MeOH): m/z $[M+H]^+$, calcd for $C_{56}H_{76}N_7O_{13}$ 1054.5501; found 1054.5524, m/z $[M+Na]^+$, calcd for $C_{56}H_{75}N_7O_{13}Na$ 1076.5321; found 1076.5360; HPLC purity: TR (α,β) = 18.77, 19.24 min., 96.1 %.

Benzyl *N*-[(5*S*)-6-[2-(5-acetamido-2-methoxy-benzoyl)hydrazino]-5-[3-[[(3*R*,4*S*,5*S*)-6-[3-[[(2S)-2-[[(2*S*)-2-aminopropanoyl]amino]-3-methyl-butanoyl]amino]propoxy]-3,4,5-tribenzyloxy-tetrahydropyran-2-yl]methoxy]propanoylamino]-6-oxo-hexyl]carbamate (23). Same procedure as described for **16a** from **19** (38 mg, 0.029 mmol) in dry CH_2Cl_2 (220 μL), to afford **23** as a white solid (35.5 mg, quantitative, α/β 50/50). R_f = 0 (CH_2Cl_2/ CH_3OH : 95/5); ^1H NMR (300 MHz, $CDCl_3$) : δ = 11.10 (sl, 1H) ; 10.65 (m, 1H); 9.52 (m, 1H); 8.50-8.01 (m, 7H); 7.32- 7.25 (m, 21H,); 6.84 (m, 1H); 5.25-4.49 (m, 11.50H, 11H+$H_{1\beta}$); 4.36 (m, 1.50H, 1H+$H_{1\alpha}$); 3.87 (s, 3H); 3.78 – 2.93 (m, 16H); 2.51 (s, 2H); 2.11 (s, 3H); 1.96- 1.81 (m, 5H); 1.50 (s, 3H); 1.44 (m, 4H); 0.88-0.85 (m, 6H) ; ^{13}C NMR (75 MHz, $CDCl_3$) : δ = 173.2, 172.0, 171.5, 171.3, 169.9, 165.5, 158.8, 153.6, 138.6, 138.2, 138.6, 138.0, 136.6, 136.5, 135.9, 133.0, 128.4,

128.3,127.9, 127.8, 127.7, 127.6, 125.8, 122.9, 117.6, 111.9, 103.9 ($C_{1H\alpha}$), 97.1 ($C_{1H\beta}$), 84.4, 82.1, 81.8, 80.0, 78.2, 77.5, 75.5, 74.9, 74.7, 74.6, 72.9, 69.6, 67.6, 66.5, 59.3, 59.1, 56.3 , 51.3, 50.0, 49.6, 40.5, 36.7, 36.5, 36.2, 32.6, 31.4, 29.2, 23.9, 22.4, 19.0, 18.4, 17.3 ; HRMS (TOF, ESI, ion polarity positive, H_2O/ MeOH): m/z $[M+H]^+$, calcd for $C_{65}H_{85}N_8O_{15}$ 1217.6134; found 1217.6168, m/z $[M+Na]^+$, calcd for $C_{65}H_{84}N_8O_{15}Na$ 1239.5954; found 1239.5972, HPLC purity: TR (α,β) = 19.24, 19.67 min., 91.1 %.

Fluorescence-detected Thioflavin-T binding assay

Thioflavin T was obtained from Sigma. $A\beta_{1-42}$ was purchased from American Peptide. The peptide was dissolved in an aqueous 1% ammonia solution to a concentration of 1 mM and then, just prior to use, was diluted to 0.2 mM with 10 mM Tris-HCl, 100 mM NaCl buffer (pH 7.4). Stock solutions of glycopeptides were dissolved in DMSO with the final concentration kept constant at 0.5% (v/v).

Thioflavin T fluorescence was measured to evaluate the development of $A\beta_{1-42}$ fibrils over time using a fluorescence plate reader (Fluostar Optima, BMG labtech) with standard 96-well black microtiter plates. Experiments were started by adding the peptide (final Aβ1-42 concentration equal to 10 μM) into a mixture containing 40 μM Thioflavin T in 10 mM Tris-HCl, 100 mM NaCl buffer (pH 7.4) with and without the tested compounds at different concentrations (100, 50, 10, 1 μM) at room temperature. The Th-T fluorescence intensity of each sample (performed in duplicate or triplicate) was recorded with 440/485 nm excitation/emission filters set for 42 hours performing a double orbital shaking of 10 s. before the first cycle. The fluorescence assays were performed between 2 and 4 times on different days, with the same batch of peptide. The ability of compounds to inhibit/accelerate Aβ1-42 aggregation was assessed considering both the time of the half-life of aggregation (t1/2) and the intensity of the

1
2
3
4
5
6
7
8
9
10
11
12
13
14
15
16
17
18
19
20
21
22
23
24
25
26
27
28
29
30
31
32
33
34
35
36
37
38
39
40
41
42
43
44
45
46
47
48
49
50
51
52
53
54
55
56
57
58
59
60

experimental fluorescence plateau (F). The relative extension (or reduction) of t1/2 is defined as the experimental t1/2 in the presence of the tested compound relative to the one obtained without the compound and is evaluated as the following percentage: t1/2(Aβ+compound) / t1/2(Aβ) x 100. The decrease (or increase) of the experimental plateau is defined as the intensity of experimental fluorescence plateau observed with the tested compound relative to the value obtained without the compound and is evaluated as the absolute value of following percentage : |FAβ - FAβ+compound| / FAβ x 100 (a decrease is indicated with a (–) and an increase with a (+).

Transmission electron microscopy

Samples were prepared under the same conditions as in the ThT-fluorescence assay. Aliquots of $A\beta_{1-42}$ (10 µM in 10 mM Tris-HCl, 100 mM NaCl NaCl, pH 7.4 in the presence and absence of the tested compounds) were adsorbed onto 300-mesh carbon grids for 2 min, washed and dried. The samples were negatively stained for 45 s. on 2 % uranyl acetate in water. After draining off the excess of staining solution and drying, images were obtained using a ZEISS 912 Omega electron microscope operating at an accelerating voltage of 80 kV.

Capillary electrophoresis

Sample preparation: the commercial $A\beta_{1-42}$ was dissolved upon reception in 0.16% NH4OH (at 2 mg/mL) for 10 minutes at 20°C, followed by an immediate lyophilization. The dried sample was then stored at -20°C until use.

CE experiments were carried out with a P/ACE TM MDQ Capillary Electrophoresis System (Beckman Coulter Inc., Brea, CA, USA) equipped with a photodiode array detector. UV Detection was performed at 190 nm. The sample (as previously described) was reconstituted by dissolution in 20 mM phosphate buffer pH 7.4 containing DMSO (control or stock solutions of

1
2
3
4
5
6
7
8
9
10
11
12
13
14
15
16
17
18
19
20
21
22
23
24
25
26
27
28
29
30
31
32
33
34
35
36
37
38
39
40
41
42
43
44
45
46
47
48
49
50
51
52
53
54
55
56
57
58
59
60

glycopeptidomimetic dissolved in DMSO). A constant DMSO/phosphate buffer ratio at 2.5% (v/v) was used for each sample. The final peptide concentration was set at 100 μM regardless the peptide/compound ratio.

For the CE separation of Aβ oligomers, fused silica capillary 60 cm (10.2 cm to the detector) 50 μm I.D. were used. The background electrolyte was a 80 mM phosphate buffer, pH 7.4. The separation was carried out under -20 kV at 25°C. The sample was injected from the outlet by hydrodynamic injection at 0.5 psi for 10 s. After each run, the capillary was rinsed for 3.5 min with NaOH 1 M, 3.5 min with water, 1 min with DMSO 10 %, 1 min with SDS 50 mM, and equilibrated with running buffer for 3 min.

NMR spectroscopy

NMR experiments were recorded on a Bruker Avance III 500 MHz spectrometer equipped with a $^{1}H/^{13}C/^{15}N$ TCI cryoprobe with Z-axis gradient. NMR spectra were processed and analysed with TopSpin software (Bruker).

The conformation of **3β** was studied in aqueous solution, either in H_2O/D_2O (90/10 v/v) or in 50 mM sodium phosphate, pH 7.4 containing 10% D_2O. ^{1}H and ^{13}C resonances were assigned using 1D ^{1}H WATERGATE, 2D ^{1}H-^{1}H TOCSY (MLEV17 isotropic scheme of 68 ms duration), 2D ^{1}H-^{1}H ROESY (500 ms mixing time), 2D ^{1}H-^{13}C HSQC, and 2D 1H-^{13}C HMBC spectra. ^{1}H and ^{13}C chemical shifts were calibrated using DSS (sodium 4,4-dimethyl-4-silapentane-1-sulfonate) as an internal reference. The ^{1}H and ^{13}C resonance assignments of **3β** are listed in Tables S1 and S2. Vicinal coupling constants were extracted from 1D ^{1}H WATERGATE. The temperature gradients of the amide proton chemical shifts were derived from 1D ^{1}H WATERGATE spectra recorded between 5 °C and 30 °C.

1
2
3
4
5
6
7
8
9
10
11
12
13
14
15
16
17
18
19
20
21
22
23
24
25
26
27
28
29
30
31
32
33
34
35
36
37
38
39
40
41
42
43
44
45
46
47
48
49
50
51
52
53
54
55
56
57
58
59
60

Samples of $A\beta_{1-42}$ in the absence or in the presence of **3β** were prepared in Shigemi tubes (280 μL volume) in 50 mM sodium phosphate, pH 7.4 containing 10% D2O. Synthetic $A\beta_{1-42}$ peptide was used in NMR experiments, with the exception of 2D HSQC experiments requiring ^{15}N, ^{13}C-labelled recombinant $A\beta_{1-42}$. Solid phase peptide synthesis of Aβ1-42 was performed at the Institut de Biologie Intégrative (IFR83- Université Pierre et Marie Curie). Recombinant $A\beta_{1-42}$ was obtained according to the protocol of Walsh et al.35 NMR experiments were acquired at 5 °C. 2D NOESY experiments were recorded with a mixing time of 0.2 s. 1D ^{1}H STD experiments were acquired using a cascade of Gaussian shaped pulses (50 ms pulse, B1 field of 0.1 kHz, total duration of 3 s) applied on resonance (–0.7 ppm) and off resonance (+30 ppm), alternatively. The number of scans was set to 320, corresponding to an experiment duration of 50 min. 1D ^{1}H WaterLOGSY (water-ligand observed via gradient spectroscopy) experiments were recorded using a Gaussian pulse of 20 ms duration for selective inversion of water magnetization and a mixing period of 0.5 s. The recycling delay was set to 2 s and the total number of scans was 1200, corresponding to an experimental time of 1 hour.

SPR experiments

For these studies we used the Biacore T100 (GE Healthcare, France) apparatus, which has 4 parallel flow channels. $A\beta_{1-42}$ peptide was immobilized on the carboxy-terminated dextran matrix on gold surface sensor chip (CM5 sensor chip, GE Healthcare, France) by an optimized amine coupling method. Briefly, the surface was treated with a mixture of 0.4 M EDC and 0.1 M NHS (1/1) in water for 7 min. at 10 μL/min. Then, a freshly prepared $A\beta_{1-42}$ solution (0.05 μM) in a 10 mM sodium acetate buffer (pH 4.6) was injected 4 times during 15 min. each at 10 μL/min on the NHS-activated surface. Then, a final injection of ethanolamine was done to block the non-linked activated amine. A reference surface was prepared using the same immobilization

procedure but with an ethanolamine injection instead of the peptide (blank surface). At that point of the process, the fixation lead to a SPR signal of 3000 RU. A rinsing step using an aqueous solution of $NH_4OH.H_2O$ 0.1 % (9 injections of 1 min. each at 30 µL/min.) was performed in order to remove from the surface all the $A\beta_{1-42}$ aggregates that may have been formed during the immobilization step. After these rinsing steps, the chip gave a signal of about 1500 RU.

Binding of compounds **3β**, **1** and curcumin to $A\beta_{1-42}$ fixed on the SPR chips : Solutions of compounds in 150 mM PBS containing 2% DMSO solubilized in DMSO were injected on the $A\beta_{1-42}$ surface for 1 min. at 80 µL/min. The rinsing step was performed using the running buffer for 5 min. and the regeneration step using the aqueous solution of $NH_4OH.H_2O$ 0.1 % (3 times for 5 min at 30 µL/min.). The range of concentrations started from 12.5 µM and ended at 200 µM in PBS (150 mM), 2% DMSO. A DMSO solvent correction was applied to the raw signals and non-specific signal was subtracted using the blank channel.

Cell toxicity

SH-SY5Y neuroblastoma cells were grown in low serum Optimem (Life Technologies) for 24 hours at 37˚C, 5% CO2 in a 96 well plate at 20 000 cells per well. $A\beta_{1-42}$ was dissolved in sterile PBS at 50 µM concentration in the presence of 1, 5, 10 and 50 µM of either **1** or **3** for 24 hours at room temperature, along with a control incubation with no inhibitor. After the 24 hour period, media was removed from the cells and replaced with Optimem containing the pre-incubated $A\beta_{1-42}$ plus inhibitor diluted one in ten (5 µM Aβ final concentration) in quadruplicate. The cells were incubated for a further 24 hours as before and the cell viability (MTS assay) and cell proliferation (LDH assay) assessed using the CellTiter 96® Aqueous One Solution Cell Proliferation Assay (Promega) and CytoTox 96® Non-Radioactive Cytotoxicity Assay (Promega) respectively. The assays were repeated twice and representative samples are shown.

1
2
3
4
5
6
7
8
9
10
11
12
13
14
15
16
17
18
19
20
21
22
23
24
25
26
27
28
29
30
31
32
33
34
35
36
37
38
39
40
41
42
43
44
45
46
47
48
49
50
51
52
53
54
55
56
57
58
59
60

Plasma stability

Both **1** and **3** were dissolved at 40 μM in DMSO and then diluted to 1 μM in 10% human plasma, 90% sterile PBS. One hundred microlitre samples were run on an HPLC system (Dionex, with C18 Jupiter column from Phenomenex) using a gradient of 0-80%B (Buffer A: 0.1% trifluoroacetic acid in water, Buffer B: 0.05% trifluoroacetic acid in acetonitrile). Samples were monitored at 230 nm. After 24 hour incubation at 37˚C 100 μL samples were run on the same gradient and monitored as before.

ASSOCIATED CONTENT

Supporting Information. NMR assignments of **3β**; representative NMR spectra and HPLC purities, experimental procedure for fluorescence-detected ThT binding assay on $A\beta_{1-42}$ and IAPP; representative curves of ThT fluorescence assays; experimental procedure for TEM, CE, NMR and SPR.

AUTHOR INFORMATION

Corresponding Author

* E-mail : Sandrine.ongeri@u-psud.fr.

Phone : +33 1 46 83 57 37.

Author Contributions

The manuscript was written through contributions of all authors. All authors have given approval to the final version of the manuscript.

1
2
3
4
5
6
7
8
9
10
11
12
13
14
15
16
17
18
19
20
21
22
23
24
25
26
27
28
29
30
31
32
33
34
35
36
37
38
39
40
41
42
43
44
45
46
47
48
49
50
51
52
53
54
55
56
57
58
59
60

Funding Sources

The Ministère de l'Enseignement Supérieur et de la Recherche (MESR) is thanked for financial support for DB. The European Union is thanked for funding the research training of NT, KF, CB and YI in the frame of the European student exchange Erasmus programme.

The Laboratory BioCIS is a member of the Laboratory of Excellence LERMIT supported by a Grant from ANR (ANR-10-LABX-33).

ACKNOWLEDGMENT

Chiara Bernardi (CB) (BioCIS, UMR 8076) is thanked for her help with the synthesis. Claire Troufflard and Karine Leblanc (BioCIS, UMR 8076) are thanked for their help with the NMR experiments and the HPLC analysis respectively. Magali Noiray (CIBLOT-Bia, Université Paris-Sud) and Géraldine Toutirais (Institut de Biologie Paris Seine (IBPS)/ FR3631, Service de Microscopie Electronique, Université Pierre et Marie Curie, France) are acknowledged for their advices in SPR and TEM experiments respectively.

ABBREVIATIONS

Aβ, Amyloid-beta peptide; AD, Alzheimer's disease; CE, Capillary Electrophoresis; STD, Saturation Transfer Difference; ThT, Thioflavin T; TEM, Transmission Electron Microscopy; SPR, Surface Plasmon resonance; SAR, Structure-activity relationships; DMTMM, [4-(4,6-Dimethoxy1,3,5-triazin-2-yl)-4-methyl-morpholinium tetrafluoroborate]; DMAP, 4-dimethylaminopyridine.

1
2
3
4
5
6
7
8
9
10
11
12
13
14
15
16
17
18
19
20
21
22
23
24
25
26
27
28
29
30
31
32
33
34
35
36
37
38
39
40
41
42
43
44
45
46
47
48
49
50
51
52
53
54
55
56
57
58
59
60

REFERENCES

(1) (a) Alzheimer's disease international. World Alzheimer Reports. http://www.alz.co.uk/research/world-report (accessed december 14th, 2015). (b) Mucke, L. Neuroscience : Alzheimer's disease. *Nature* **2009**, *461*, 895-897.

(2) (a) Goedert, M.; Spillantini, M. G. A Century of Alzheimer's Disease. Science **2006**, *314*, 777-780. (b) Haas, C. ; Selkoe, D. J. Soluble protein oligomers in neurodegeneration : lessons from the Alzheimer amyloid β-peptide. *Nat. Rev. Mol. Cell Biol.* **2007**, *8*, 101-112.

(3) Cohen, S. I. A.; Linse, S.; Luheshi, M.; Hellstrand, E.; White, D. A.; Rajah, L.; Otzen, D. L.; Vendruscolo, M.; Dobson, C. M.; Knowles, T. P. J. Proliferation of amyloid-β42 aggregates occurs through a secondary nucleation mechanism. *Proc. Natl. Acad. Sci. USA.* **2013**, *110*, 9758-9763.

(4) Matsumura, S.; Shinoda, K.; Yamada, M.; Yokojima, S.; Inoue, M.**;** Ohnishi, T; Shimada, T.; Kikuchi, K.; Masui, D.; Hashimoto, S.; Sato, M.; Ito, A.; Akioka, M.; Takagi, S.; Nakamura, Y.; Nemoto, K.; Hasegawa, Y.; Takamoto, H.; Inoue, H.; Nakamura, S.; Nabeshima,Y.; Teplow, D.B.; Kinjo, M.; Hoshi, M. Two distinct amyloid β-protein (Aβ) assembly pathways leading to oligomers and fibrils identified by combined fluorescence correlation spectroscopy, morphology, and toxicity analyses. *J. Biol. Chem.* **2011**, *286*, 11555-11562.

(5) Jeong, J. S.; Ansaloni, A.; Mezzenga, R.; Lashuel, H. A.; Dietler, G. Novel mechanistic insight into the molecular basis of amyloid polymorphism and secondary nucleation during amyloid formation. *J. Mol. Biol.* **2013,** *425,* 1765-1781.

1
2
3
4
5
6
7
8
9
10
11
12
13
14
15
16
17
18
19
20
21
22
23
24
25
26
27
28
29
30
31
32
33
34
35
36
37
38
39
40
41
42
43
44
45
46
47
48
49
50
51
52
53
54
55
56
57
58
59
60

(6) Lührs, T.; Ritter, C.; Adrian, M.; Riek-Loher, D.; Bohrmann, B.; Döbeli, H.; Schubert, D.; Riek, R. 3D structure of Alzheimer's amyloid-β(1-42) fibrils. *Proc. Natl. Acad. Sci. USA.* **2005**, *102*, 17342-17347.

(7) Laganowsky, A.; Liu, C.; Sawaya, R. M.; Whitelegge, J. P.; Park, J.; Zhao, M. Atomic view of a toxic amyloid small oligomer. *Science* **2012**, *335*, 1228-1231.

(8) Yu, L.; Edalji, R.; Harlan, J. E.; Holzman, T. F.; Pereda Lopez, A.; Labkovsky, B.; Hillen, H.; Barghorn, S.; Ebert, U.; Richardson, P.L.; Miesbauer; L.; Solomon, L.; Bartley, D.; Walter, K.; Johnson, R.W.; Hajduk, P.J.and Olejniczak, E.T. Structural characterization of a soluble amyloid β-peptide oligomer. *Biochemistry* **2009**, *48*, 1870-1877.

(9) Ahmed, M.; Davis, J.; Aucoin, D.; Sato, D.; Ahuja, S.; Aimoto, S.; Elliott, J. J.; Van Nostrand W. E.; O Smith. Structural conversion of neurotoxic amyloid-β1-42 oligomers to fibrils. *Nat. Struct. Mol. Biol.* **2010**, *17,* 561-567.

(10) Wälti M. A.; Orts J.; Vçgeli B.; Campioni S.; Riek R. Solution NMR Studies of recombinant Aβ(1–42): from the presence of a micellar entity to residual β-sheet structure in the soluble species. *ChemBioChem* **2015**, *16*, 659-669.

(11) Dahlgren, K. N.; Manelli, A. M.; Blaine Stine, W.; Baker, L. K.; Krafft, G. A; LaDu, M. J. Oligomeric and fibrillar species of amyloid-β peptides differentially affect neuronal viability. *J. Biol. Chem.* **2002**, *277*, 32046-32053.

(12) Jan, A.; Gokce, O.; Luthi-Carter R.; Lashuel, H. A. The ratio of Monomeric to Aggregated forms of Aβ40 and Aβ42 is an important determinant of amyloid-β aggregation, fibrillogenesis, and toxicity. *J. Biol. Chem.* **2008**, *283*, 28176-28189.

1
2
3
4
5
6
7
8
9
10
11
12
13
14
15
16
17
18
19
20
21
22
23
24
25
26
27
28
29
30
31
32
33
34
35
36
37
38
39
40
41
42
43
44
45
46
47
48
49
50
51
52
53
54
55
56
57
58
59
60

(13) Ono, K.; Condron, M. M.; Teplow, D. B. Structure-neurotoxicity relationships of amyloid β-protein oligomers. *Proc. Natl. Acad. Sci. USA.* **2009**, *106*, 14745-14750.

(14) Shankar, G. M.; Li, S.; Mehta, T. H.; Garcia-Munoz A.; Shepardson, N. E.; Smith I.; Brett, F.M.; Farrell, M.A.; Rowan, M.J.; Lemere, C.A.; Regan; C.M.; Walsh, D.M.; Sabatini, B.L. and Selkoe, D.J. Amyloid β-protein dimers isolated directly from Alzheimer brains impair synaptic plasticity and memory. *Nat. Med.* **2008**, *14,* 837-842.

(15) Prangkio, P.; Yusko, E. C.; Sept, D.; Yang, J.; Mayer, M. Multivariate analyses of amyloid-beta oligomer populations indicate a connection between pore formation and cytotoxicity. *PLoS ONE* **2012**, *7*, 47261.

(16) Cizas, P.; Budvytyte, R.; Morkuniene, R.; Moldovan, R.; Broccio, M.; Lösche, M.; Niaura, G.; Valincius, G.; Borutaite,V. Size-dependent neurotoxicity of β-amyloid oligomers. *Arch. Biochem. Biophys.* **2010**, *496*, 84-92.

(17) Mayes, J.; Tinker-Mill, C.; Kolosov, O.; Zhang, H.; Tabner, B. J.; Allsop, D. β-Amyloid fibrils in Alzheimer's disease are not inert when bound to copper ions but can degrade hydrogen peroxide and generate reactive oxygen species. *J Biol Chem.* **2014**, *289*, 12052-12062.

(18) Cohen, S. I. A.; Linse, S.; Luheshi, L. M.; Hellstrand, E.; White, D. A.; Rajah, L.; Otzen, D. E.; Vendruscolo, M.; Dobson, C. M.; Knowles, T. P. J. Proliferation of amyloid-β42 aggregates occurs through a secondary nucleation mechanism. *Proc Natl Acad Sci U S A.* ***2013**, 110, 9758*-9763.

(19) (a) Belluti, F.; Rampa, A.; Gobbi, S.; Bisi, A. Small-molecule inhibitors/modulators of amyloid-β peptide aggregation and toxicity for the treatment of Alzheimer's disease: a patent

review (2010 - 2012). *Expert Opin. Ther. Pat.* **2013**, *23*, 581-596. (b) Härd, T.; Lendel, C. Inhibition of amyloid formation. *J. Mol. Biol.* **2012**, *421*, 441–465. (c) Doig, A. J.; Derreumaux P. Inhibition of protein aggregation and amyloid formation by small molecules. *Curr. Opin. Struct. Biol.* **2015**, *30*, 50-56.

(20) (a) Stains, C.I.; Mondal, K.; Ghosh, I. Molecules that target beta-Amyloid. *ChemMedChem.* **2007**, *2*, 1674-1692. (b) Takahashi, T.; Mihara, H. Mimetics. Peptide and protein mimetics inhibiting amyloid peptide aggregation. *Acc. Chem. Res.* **2008**, *41*, 1309-1318. (c) Neddenriep, B.; Calciano, A.; Conti, D.; Sauve, E.; Paterson, M.; Bruno, E.; Moffet, D. A. Short peptides as inhibitors of amyloid aggregation. *Open Biotechnol. J.* **2011,** *5*, 39-46. (d) Luo, J.; Abrahams. J. P. Cyclic peptides as inhibitors of amyloid fibrillation. *Chem. Eur. J.* **2014**, *20*, 2410-2419.

(21) Cheng, P.-N.; Liu, C.; Zhao, M.; Eisenberg, D.; Nowick, J. S. Amyloid β-sheet mimics that antagonize protein aggregation and reduce amyloid toxicity. *Nat. Chem.* **2012**, *4*, 927-933.

(22) Taylor, M.; Moore, S.; Mayes, J.; Parkin, E.; Beeg, M.; Canovi, M.; Gobbi, M.; Mann, D. M. A.; Allsop, D. Development of a proteolytically stable retro-inverso peptide inhibitor of β-amyloid oligomerization as a potential novel treatment for Alzheimer's disease. *Biochemistry* **2010**, *49*, 3261-3272.

(23) Arai, T.; Araya, T.; Sasaki, D.; Taniguchi, A.; Sato, T.; Sohma, Y.; Kanai, M. Rational Design and identification of a non-peptidic aggregation inhibitor of amyloid-β based on a pharmacophore motif obtained from cyclo[-Lys-Leu-Val-Phe-Phe-]. *Angew. Chem. Int. Ed.* **2014**, 53, 8236-8239.

1
2
3
4
5
6
7
8
9
10
11
12
13
14
15
16
17
18
19
20
21
22
23
24
25
26
27
28
29
30
31
32
33
34
35
36
37
38
39
40
41
42
43
44
45
46
47
48
49
50
51
52
53
54
55
56
57
58
59
60

(24) (a) Dorgeret, B.; Khémtemourian, L.; Correia, I.; Soulier, J-L; Lequin, O. ; Ongeri, S. Sugar-based peptidomimetics inhibit amyloid β-peptide aggregation. *Eur. J. Med. Chem.* **2011**, *46*, 5959-5969. (b) Kaffy, J.; Brinet, D.; Soulier, J-L; Khemtémourian, L.; Lequin, O.; Taverna, M.; Crousse, B.; Ongeri, S. Structure-activity relationships of sugar-based peptidomimetics as modulators of amyloid β-peptide early oligomerization and fibrillization. *Eur. J. Med. Chem.* **2014**, *86*, 752-758.

(25) (a) Gruner, S. A. W.; Truffault, V.; Voll, G.; Locardi, E.; Stöckle, M.; Kessler, H. Design, Synthesis, and NMR structure of linear and cyclic oligomers containing novel furanoid sugar amino acids. *Chem. Eur. J.* **2002**, *8*, 4366-4376. (b) Schweizer, F. Glycosamino acids: building blocks for combinatorial synthesis–implications for drug discovery. *Angew. Chem. Int. Ed.* **2002**, *41*, 230-253. (c) Risseueuw, M. D. P.; Overhand, M.; Fleet, G. W. J.; Simone, M. I. A compendium of sugar amino acids (SAA): scaffolds, peptide- and glyco-mimetics. *Tetrahedron: Asymmetry* **2007**, *18*, 2001-2010.

(26) Nowick, J. S.; Chung, D. M.; Maitra, K.; Maitra, S.; Stigers, K. D.; Sun, Y. An unnatural amino acid that mimics a tripeptide β-strand and forms β-sheet like hydrogen-bonded dimers. *J. Am. Chem. Soc*. **2000**, *122*, 7654-7661.

(27) (a) Bannwarth, L.; Kessler, A.; Pèthe, S.; Collinet, B.; Merabet, N.; Boggetto, N.; Sicsic, S.; Reboud-Ravaux, M.; Ongeri, S. Molecular tongs containing amino acid mimetic fragments : new inhibitors of wild-type and mutated HIV-1 protease dimerization. *J. Med. Chem*. **2006**, *49*, 4657-4664. (b) Vidu, A.; Dufau, L.; Bannwarth, L.; Soulier, J-L; Sicsic, S.; Piarulli, U.; Reboud-Ravaux, M.; Ongeri, S. Towards the first non peptidic molecular tong inhibitor of wild-type and mutated HIV-1 protease dimerization. *ChemMedChem* **2010**, *5*, 1899-1906.

1
2
3
4
5
6
7
8
9
10
11
12
13
14
15
16
17
18
19
20
21
22
23
24
25
26
27
28
29
30
31
32
33
34
35
36
37
38
39
40
41
42
43
44
45
46
47
48
49
50
51
52
53
54
55
56
57
58
59
60

(28) (a) Yamanoi, T.; Inoue, R.; Matsuda, S.; Iwao, K.; Oda, Y.; Yoshida, A.; Hamasaki, K. Formation of O-glycosidic linkages from 1-hydroxy sugars by bismuth(III) triflate-catalyzed dehydrative glycosidation. *Heterocycles* **2009**, *77*, 445-460. (b) Yamazaki, T.; Sugawara, F.; Ohta, K.; Masaki, K.; Nakayama, K.; Sakaguchi, K.; Sato, N.; Sahara, H.; Fujita, T. Novel sulfoquinovosylacylglycerol derivative, and use thereof as medicaments. *US. Patent Appl. Publ.* **2002**, US 20020052327 A1.

(29) (a) Kaminski, Z.J.; Kolesinska B.; Kolesinska, J.; Sabatino, G.; Chelli, M.; Rovero, P.; Błaszczyk, M.; Głowka, M.L.; and Papini, A.M. N-Triazinylammonium tetrafluoroborates. A new generation of efficient coupling reagents useful for peptide synthesis. *J. Am. Chem. Soc.* **2005**, *127*, 16912-16920. (b) Jastrzabek K.G.; Subiros-Funosas, R.; Albericio, F.; Kolesinska, B.; and Kaminski , Z.J. 4-(4,6-Di[2,2,2-trifluoroethoxy]-1,3,5-triazin-2-yl)-4-methylomor-pholinium tetrafluoroborate. Triazine-based coupling reagents designed for coupling sterically hindered substrates. *J. Org. Chem.* **2011**, *76*, 4506-4513.

(30) Komarova, B. S.; Maryasina, S. S.; Tsvetkov, Y. E.; Nifantiev, N. E. Water-dependent reduction of carbohydrate azides by dithiothreitol. *Synthesis* **2013**, *45*, 471-478.

(31) LeVine 3rd, H. Quantification of β-sheet amyloid fibril structures with thioflavin T. *Methods Enzymol.* **1999**, *309*, 274-284.

(32) Brinet, D.; Kaffy, J.; Oukacine, F.; Glumm, S.; Ongeri, S.; Taverna, M. An improved CE method for the in vitro monitoring of the challenging early steps of the $A\beta_{1-42}$ peptide oligomerization: application to anti-Alzheimer's drug discovery. *Electrophoresis* **2014**, *35,* 3302-3309.

(33) Fawzi, N.L.; Ying, J.; Ghirlando, R.; Torchia, D.A.; Clore, G.M. Atomic-resolution dynamics on the surface of amyloid-β protofibrils probed by solution NMR. *Nature* **2011**, *480*, 268-272.

(34) Walsh, D.M.; Thulin, E.; Minogue, A.M.; Gustavsson, N.; Pang, E.; Teplow, D.B.; Linse, S. A facile method for expression and purification of the Alzheimer's disease-associated amyloid β-peptide. *FEBS J.* **2009**, *276*, 1266-1281.

(35) Airoldi, C.; Cardona, F.; Sironi, E.; Colombo, L.; Salmona, M.; Silva, A.; Nicotra, F.; La Ferla, B. cis-Glyco-fused benzopyran compounds as new amyloid-β peptide ligands. *Chem. Commun.* **2011**, *47*, 10266-10268.

(36) Taniguchi, A.; Sohma, Y.; Hirayama, Y.; Mukai, H.; Kimura, T.; Hayashi, Y.; Matsuzaki, K.; Kiso, Y. "Click peptide": pH-triggered in situ production and aggregation of monomer Abeta1-42. *ChemBioChem* **2009**, *10*, 710-715.

(37) Canovi, M.; Lucchetti, J.; Stravalaci, M.; Re, F.; Moscatelli, D.; Bigini, P.;Salmona, M.; Gobbi, M. Applications of surface plasmon resonance (SPR) for the characterization of nanoparticles developed for biomedical purposes. *Sensors* **2012**, *12*, 16420-16432.

(38) (a) Amijee, H.; Bate, C.; Williams, A.; Virdee, J.; Jeggo, R.; Spanswick, D.; Scopes, D.I.C.; Treherne, J.M.; Mazzitelli, S.; Chawner, R.; Eyers, C.E.; Doig, A.J. The N-methylated peptide SEN304 powerfully inhibits Aβ(1–42) toxicity by perturbing oligomer formation. *Biochemistry* **2012**, *51*, 8338-8352. (b) Maezawa, I.; Hong, H-S.; Liu, R.; Wu, C-Y.; Cheng, R-H.; Kung, M-P.; Kung, H.F.; Lam, K.S.; Oddo, S.; LaFerla, F.M.; Jin, L-W. Congo red and thioflavin-T analogs detect Aβ oligomers. *J. Neurochem.* **2008**, *104*, 457-468.

(39) Stravalaci, M.; Bastone, A. ; Beeg, M.; Cagnotto, A.; Colombo, L.; Di Fede, G.; Tagliavini, F.; Cantù, L.; Del Favero, E.; Mazzanti, M.; Chiesa, R.; Salmona, M.; Diomede, L.; Gobbi, M. Specific recognition of biologically active amyloid-β oligomers by a new surface plasmon resonance-based immunoassay and an in vivo assay in Caenorhabditis elegans. *J. Biol. Chem.* **2012**, *287*, 27796-27805.

(40) Kai, T.; Zhang, L.; Wang, X.; Jing, A.; Zhao, B.; Yu, X.; Zheng, J.; Zhou, F. Tabersonine inhibits amyloid fibril formation and cytotoxicity of Aβ(1–42). *ACS Chem. Neurosci.* **2015**, 6, 879-888.

(41) Yang, F.; Lim, G-P.; Begum, A-N.; Ubeda, O-J.; Simmons, M-R.; Ambegaokar, S-S.; Chen, P-P.; Kayed, R.; Glabe, C-G.; Frautschy, S-A.; Cole, G-M. Curcumin inhibits formation of amyloid β oligomers and fibrils, binds plaques, and reduces amyloid *in vivo*. *J. Biol. Chem*. **2005**, *280*, 5892-5901.

(42) (a) Smith, M.D.; Cruz, L. Changes to the structure and dynamics in mutations of Aβ21−30 caused by ions in solution. *J. Phys. Chem. B* **2013**, *117,* 14907-14915. (b) Hochdörffer, K.; März-Berberich, J.; Nagel-Steger, L.; Epple, M.; Meyer-Zaika, W.; Horn, A.H.C.; Sticht, H.; Sinha, S.; Bitan, G.; Schrader, T. Rational design of β-sheet ligands against Aβ42-induced toxicity. *J. Am. Chem. Soc.* **2011**, *133*, 4348-4358.

(43) Feng, Y.; Wanga, X.-P.; Yang, S.-G.; Wan, Y.-J.; Xi Zhang, Du, X.-T.; Sun, X.-X.; Zhao, M.; Huang, L.; Liu, R.-T. Resveratrol inhibits beta-amyloid oligomeric cytotoxicity but does not prevent oligomer formation. *Neurotoxicology* **2009**, *30*, 986-995.

(44) Sinha, S.; Du, Z.; Maiti, P.; Klärner, F.-G.; Schrader, T.; Wang, C.; Bitan. G. Comparison of Three Amyloid Assembly Inhibitors: The sugar *scyllo*-inositol, the polyphenol epigallocatechin gallate, and the molecular tweezer CLR01. *ACS Chem. Neurosci*. **2012**, *3*, 451-458.

(45) Hyunga, S.-J.; DeTomaa, A. S.; Brendera, J. R.; Leec, S.; Vivekanandana, S.; Kochia, A.; Choic, J.-S.; Ramamoorthya, A.; Ruotoloa, B. T.; Lima, M. H. Insights into anti-amyloidogenic properties of the green tea extract (−)-epigallocatechin-3-gallate toward metal-associated amyloid-β species. *Proc. Natl. Acad. Sci. USA*. **2013**, *110*, 3743-3748.

(46) Bieschke, J.; Herbst, M.; Wiglenda, T.; Friedrich, R. P.; Boeddrich, A.; Schiele, F.; Kleckers, D.; Lopez del Amo, J. M.; Grüning, B. A.; Wang, Q.; Schmidt, M. R.; Lurz, R.; Anwyl, R.; Schnoeg, S.; Fändrich, M.; Frank, R. F.; Reif, B.; Günther, S.; Walsh, D. M.; Wanker, E. E. Small-molecule conversion of toxic oligomers to nontoxic β-sheet–rich amyloid fibrils. *Nat. Chem. Biol.* **2012**, *8*, 93-101.

1
2
3
4
5
6
7
8
9
10
11
12
13
14
15
16
17
18
19
20
21
22
23
24
25
26
27
28
29
30
31
32
33
34
35
36
37
38
39
40
41
42
43
44
45
46
47
48
49
50
51
52
53
54
55
56
57
58
59
60

For Table of Contents Only